Chapter 7
Acoustic Emission

Dimitrios G. Aggelis, Markus G. R. Sause, Pawel Packo, Rhys Pullin, Steve Grigg, Tomaž Kek, and Yu-Kun Lai

Abstract Acoustic emission (AE) is one of the most promising methods for structural health monitoring (SHM) of materials and structures. Because of its passive and non-invasive nature, it can be used during the operation of a structure and supply information that cannot be collected in real time through other techniques. It is based on the recording and study of the elastic waves that are excited by irreversible processes, such as crack nucleation and propagation. These signals are sensed by transducers and are transformed into electric waveforms that offer information on the location and the type of the source. This chapter intends to present the basic principles, the equipment, and the recent trends and applications in aeronautics, highlighting the role of AE in modern non-destructive testing and SHM. The literature in the field is vast; therefore, although the included references provide an idea of the basics and the contemporary interest and level of research and practice, they are just a fraction of the total possible list of worthy studies published in the recent years.

D. G. Aggelis (✉)
Vrije Universiteit Brussel, Brussels, Belgium
e-mail: Dimitrios.Aggelis@vub.be

M. G. R. Sause
Institute of Materials Resource Management, University of Augsburg, Augsburg, Germany

P. Packo
AGH University of Science and Technology, Krakow, Poland

R. Pullin · S. Grigg · Y.-K. Lai
Cardiff University, Cardiff, UK

T. Kek
University of Ljubljana, Ljubljana, Slovenia

7.1 Introduction

The safety of structures is of paramount importance. Operational loads, environmental influences and random phenomena such as impacts accumulate damage and compromise the durability of structures. To avoid human casualties as well as loss of capital, structural health monitoring (SHM) procedures are implemented in all fields of engineering, including aeronautics. These procedures involve detection, geometric localization and characterization of damage that allows proper engineering decisions concerning maintenance or replacement of the component. Because of the deterioration of materials and structures, the necessity for suitable inspection and maintenance is crucial. In addition, AE is a valuable tool in any platform for investigation and development of materials in laboratory conditions. It can be applied in intervals or continuously to supply the information in real time as well as a reliable evaluation of the damage condition in materials and structures (Prosser 2002). AE is a monitoring technology that offers certain advantages in the evaluation of materials as well as structures. Some of the basic features include the high sensitivity, which leads to the detection of the actual onset of micro-cracking and the possibility of characterization of the failure mode based on the recorded waveform. In addition, it offers the localization of the sources in one, two or three dimensions.

The sensitivity of AE is demonstrated if we consider that the absolute energy of AE signals is measured with the unit of atto-Joule (or 10^{-18}J!). Therefore, the method allows the detection of the actual initiation of micro-cracking or any other event that would be impossible to detect through other techniques. It is characteristic that a common mosquito of mass 2.5 mg, flying at a speed of 10 cm/s obtains a kinetic energy of approximately 1.25×10^{-8} J, which is already 10 orders of magnitude higher than the limit of the technique (Fig. 7.1).

Fig. 7.1 The amount of energy that can be measured via AE systems is 10 orders of magnitude lower than the kinetic energy of a mosquito
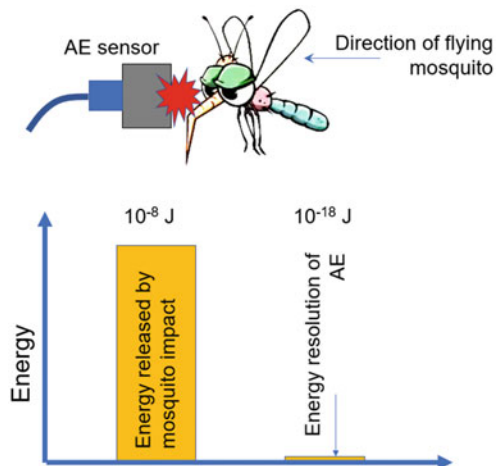
Another advantage is the potential to characterise the fracture mode or generally the source or excitation type. This may seem to some as a 'detail', since for many people, the fact that damage exists is important, disregarding the actual mode. However, for composites the mode of the crack in a matrix or the type of failure, such as delamination or fiber pull-out is indicative of the current deterioration stage, and thus, it allows projections on the useful life of the component. This mode characterization is due to the fact that distinct processes involve different motions of the crack tips and emit elastic waveforms with different characteristics. A common example is the fracture of fibrous composite materials. At low load or fatigue cycles, the matrix is expected to crack first. Then, as loading progresses, the density of debonding and pull-out events will increase, whereas eventually, fiber rupture is also possible. The analysis of the waveforms recorded at each loading stage enables the classification of the signals to the different original sources and the evaluation of the current operation stage.

Source localization is an additional strong feature of AE. By applying multiple sensors, the coordinates of the active sources can be defined with good engineering accuracy in one, two or three dimensions, which means that even if a crack is inside the volume of the material and not visible, its location can be evaluated. The localization in most cases is based on the delay of recording of successive signals of the same source event at the different sensors. Considering the material's wave speed, which can be measured using the same sensors, the location of the source can be determined. Certainly, the different wave modes excited in plate components typical in aeronautics structures, complicate the assessment, but there are strategies to overcome the difficulties, which will be explained in the corresponding section.

Because of the extensive use of AE technology in fracture monitoring studies, some people hesitate to call it a non-destructive testing technique. However, it should be clear that the AE sensors themselves do not inflict any damage (they do not even excite elastic waves as happens in ultrasonics). AE is a 'passive' technique. It is similar to filming an impact or a blast by a high-resolution camera. The camera monitors a destructive process, but it is just the monitoring tool, not the cause of damage. Because of the aforementioned advantages, AE is used for fracture monitoring, which is a very demanding and dynamic process, but it is also used for problems of different nature, e.g. the detection of gas leakage from a pipe network or corrosion development in industrial settings.

An interesting correspondence between AE and medical diagnosis is given in Wevers (1997) (see also Fig. 7.2). AE inspection is parallelised to a patient telling a doctor how she/he feels when examined without directly going into surgery to deal with the problem. The advantage of an examination over the surgery is of course that it is non-invasive and can be done for the whole body (global examination). Conversely, the disadvantage is that great skills from the doctor's side are required to interpret the surface information from the patient (or in engineering the structure) and to relate it to a specific source. In addition, the same medical condition may be manifested by different symptoms in different patients, meaning that a specific way of interpretation AE data in a material using a specific detection system may not be adequate for another material and a different detection system. In any case, AE
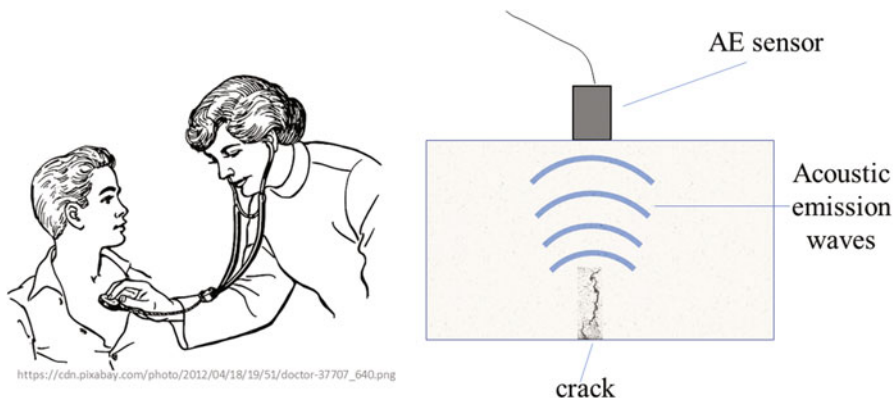
Fig. 7.2 Correspondence between medical stethoscope and AE transducer

allows continuous monitoring from the moment of damage initiation until the failure of the subject.

7.2 Basic Experimental Details and Parameters

The AE technique detects and monitors the transient elastic waves that are emitted after an irreversible phenomenon or process in the material. In most cases, piezo-electric transducers are placed on the surface of the material under test. A layer of 'couplant' or viscous liquid is applied between the sensor and the material surface to ensure adequate wave transmission. The couplant may well be petroleum jelly, or roller bearing grease. The sensors transform the pressure on their surface into electric signals. These signals are pre-amplified and are led to the digitization and acquisition board to obtain the signal as a function of time. Apart from recording the full signals, which is always an option in most contemporary systems, the basic parameters of each signal (waveform) are measured and stored as well. Figure 7.3a shows a typical AE system with the main elements, and Fig. 7.3b presents some indicative photographs of measurements.

The total activity of AE (simply how many signals or 'hits' were detected) is indicative of the phenomenon under monitoring. In case this is fracture, the number of hits is related to the damage degree and the rate of crack formation and propagation. In addition, the shape of the waveform yields important information relative to the source of the emission. The early AE systems, with no capacity for recording full waveforms, extracted only a set of features indicative of the waveform shape that were also useful for source characterization. Therefore, several parameters are used for the quantification of the waveform. Figure 7.4 shows some of the most basic ones (a, time, and b, frequency domain).
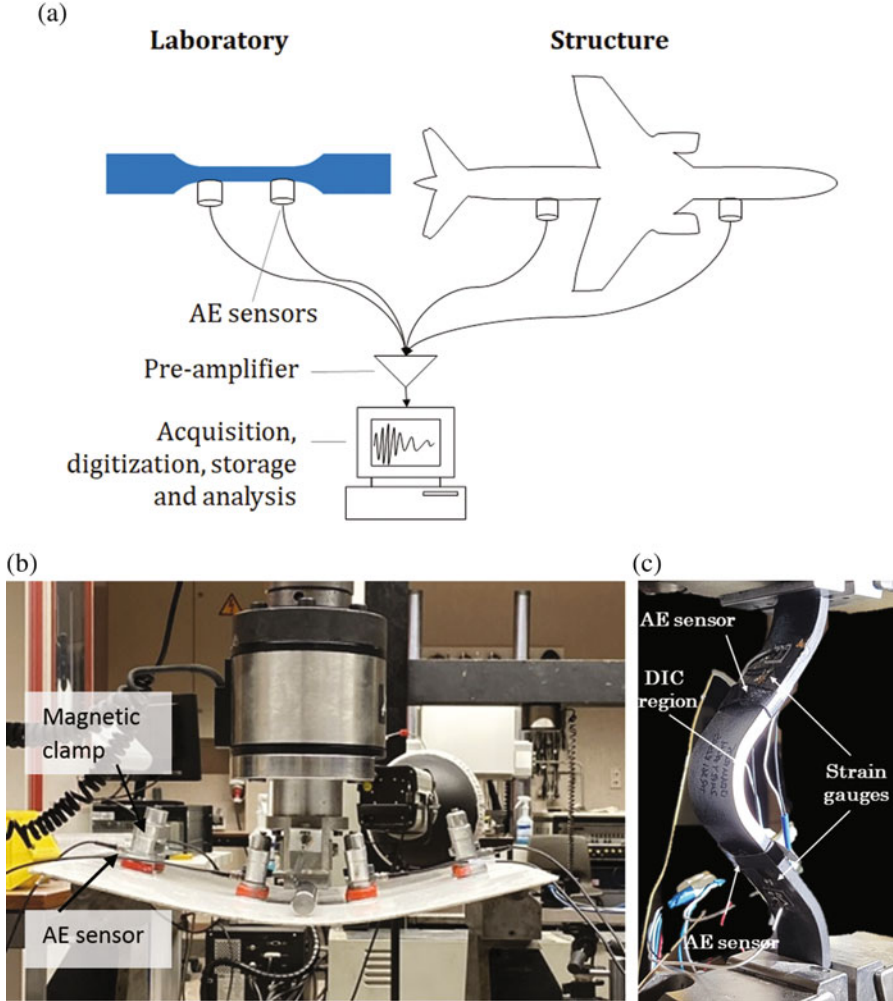
Fig. 7.3 (**a**) Schematic representation of a typical AE system, (**b**) photograph during three-point bending testing of glass fiber plate (Ospitia et al. 2020) with four AE sensors, and (**c**) tensile test of curved carbon fiber composite with AE monitoring by two sensors and digital image correlation (DIC) (Murray et al. 2020)

A basic experimental setting is the 'threshold', which is a voltage that should be overpassed to trigger the acquisition. This is an easy way to avoid low amplitude noise (extraneous AE, for example from rubbing) and is relevant to the measurement of most parameters. A parameter that is related to the intensity of the phenomenon is amplitude (A). This is the voltage (V) of the highest peak of the waveform and can also be measured in decibels (dB). dB is defined as:
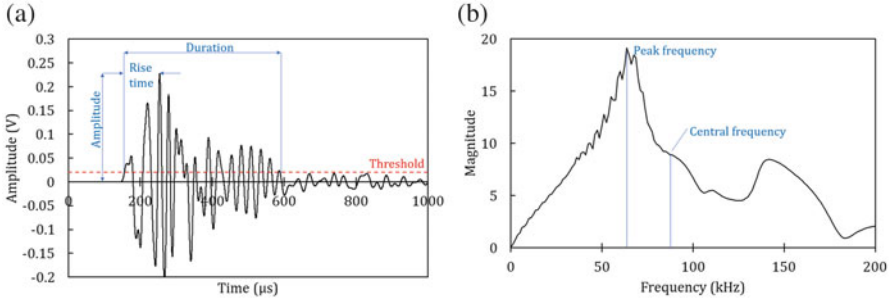
Fig. 7.4 (**a**) Typical AE waveform with basic AE parameters and (**b**) fast Fourier transform with basic spectral parameters

$$dB = 20 \cdot \log \left(\frac{A}{A_{ref}} \right) \tag{7.1}$$

where A is the measured voltage and A_{ref} a constant reference value.

Additionally, energy (E) which is defined as the measured area under the rectified signal envelope, considers the content of the whole waveform. Another definition of energy, 'absolute energy', comes from the integration of the rectified waveform envelope squared and is measured in 'attoJoule'. It is considered analogous to the energy released from the source:

$$E_{abs} = \int_0^{t_1} V^2(t) dt \tag{7.2}$$

where the waveform starts at time 0 and ends at t_1.

The delay between the first threshold crossing and the highest peak is called signal rise time, RT. Duration (Dur) is defined as the delay between the first and the last threshold crossings. Based on the shape of the first part of the waveform, the RA value has been introduced, which is defined by RT over A and is the inverse of the opening slope of the waveform or 'Grade' (Philippidis et al. 1998). The frequency content is also important. Different parameters are used for the process of this field of information. The simplest is the average frequency (AF) that is calculated in the time domain as the ratio of the total number of threshold crossings (counts) over the duration of the waveform in kHz. Other parameters such as the peak frequency and the central frequency are calculated in the frequency domain. The former is the frequency with the highest magnitude, and the latter is the centroid of the spectrum (see Fig. 7.4b). To measure these features, the full waveform should be recorded (Grosse and Linzer 2008). Parameters including the energy, RT, Dur, RA and frequency content exhibit sensitivity to fracture sources and are used for fracture mode characterization as will be discussed in more detail below. Practically, the initial part of the waveform contains information more relevant to the source

mechanism, whereas the latter part may contain reflections and generally can be more strongly influenced by the geometry.

There are different approaches as to the analysis of data depending on the application, the setup (sensors, acquisition board) and the preference of the user. Some are based on the AE activity recorded at specific load levels. In other cases, the statistical distribution of the amplitudes is used, whereas in others, the waveform parameters are analyzed (possibly with pattern recognition tools). The treatment of full waveforms (as in 'signal based' analysis) is also very widely used; tools such as wavelets and spectral analysis are very useful in revealing hidden information of the sources.

For AE measurement systems with digitization capability, two parameters play a very important role: the 'sampling rate' and the 'dynamic range'. The sampling rate or frequency determines how dense the points within the waveform are or in other words the time lap between two successive points. For example, a sampling rate of 10 MHz means that a waveform that lasts 1 s is represented by 10,000,000 points, and consequently the points are separated by 0.1 μs. According to Nyquist theorem (Bendat and Piersol 1993), the sampling rate must be at least double than the frequency of the actual signal. In reality, to have a credible representation of the continuous signal to a digitised waveform, the sampling must be 10 times higher or even more. This will improve the credibility of any further analysis in time (localization) or frequency domain. Regarding the dynamic range, this governs the corresponding 'resolution' in the voltage scale and expresses how many different voltage readings or levels can be taken between the minimum and maximum voltage. This is given as a power of 2. For example, if the voltage of the acquisition board is 20 V peak to peak, and the number of levels is 2^{16} (16 bits) = 65536, then the resolution in voltage is 20/65536 = 0.000305 V, meaning that signals with amplitudes differing by less than this value may be measured as equal.

Examples of the application of the aforementioned and other parameters will be discussed in the following sections.

7.3   Fracture Mode Characterization in Plate Structures

Before the detailed description of the fracture mode characterization, a very basic phenomenon in AE should be reported. Its name is derived from Joseph Kaiser who was one of the pioneers of the modern AE testing. Since mechanical load is increasing in a specimen, acoustic activity is normally recorded (moderate load P1 in Fig. 7.5). If the material is unloaded and reloaded to the previous load P1, no AE is observed. This is the 'Kaiser' effect (Kaiser 1950), and the lack of recorded AE can be attributed to the fact that the damage related with the specific load level P1 has already occurred during the initial cycle. By increasing the load higher than P1 (up to P2 in Fig. 7.5), AE is again recorded since 'fresh' sources are created. Now, assuming that the load P2 caused serious damage, in the event of unloading and reloading, AE will commence at a load lower than the previous maximum
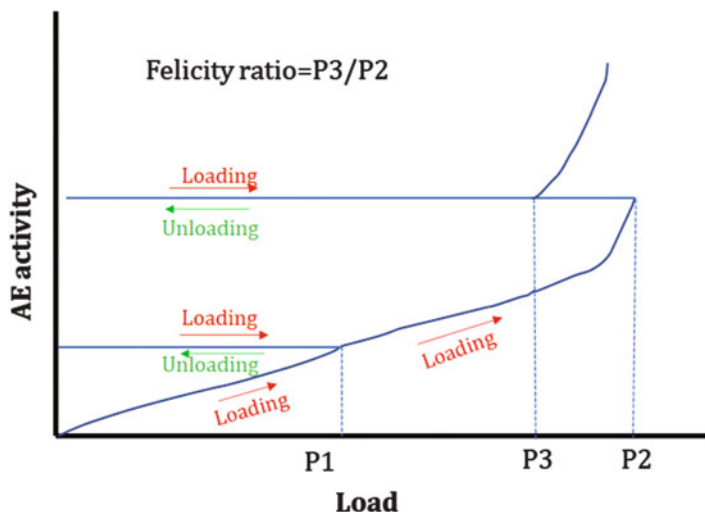
Fig. 7.5 'Kaiser effect' and Felicity ratio

(e.g. P3 < P2). This can be considered as the result of the cracks and corresponding stress concentrations that locally increase the stress even before the load reaches the previous maximum level. The load at the onset of AE, over the previous maximum load (in this case P3/P2), is called the 'Felicity' ratio (FR) (Fowler 1977). FR is close to 1 when the material is intact, meaning that the 'Kaiser effect' is valid. When the FR decreases, it indicates the accumulation of damage and is commonly used as a powerful parameter in the evaluation of composites (Hamstad 1986; Ono and Gallego 2012; Aggelis et al. 2013; Esola et al. 2018).

The Kaiser effect and FR are quite widespread in the evaluation of structural condition, but they do not directly provide information on the specific manner the material is failing (fracture mode), something that is crucial for composites. Generally, when loading a technical structure made from monolithic materials or mixed materials, the recorded AE signals will likely not originate from the same source type. A basic categorization is the distinction between 'useful' signals, such as these originating from any damage formation as outlined in Chap. 3 and 'useless' signals, such as, e.g. friction noise from the regular operation of the structure. The successful separation of these two categories is a key item to address for SHM applications and allows to focus on the portion of data that is of interest for the integrity assessment.

To understand and categorise different AE sources in materials, considering their functional principle is helpful. Basic relationships of buried AE source types, their direction of radiation and rise-time with their corresponding AE signal have been discussed in the generalised theory of acoustic emission by Ohtsu and Ono (1984, 1986). In these publications, clear emphasis is made on the importance of the source dynamics for the generation of the acoustic wave. Specifically, for crack growth, Scruby and Wadley have proposed basic relationships between the speed of crack growth, as well as directional radiation effects for metallic materials (Wadley and

Scruby 1981; Scruby 1985). These principles also apply to other materials and are therefore considered as consistent theoretical framework, which forms the baseline for various other analytical descriptions (Wadley and Scruby 1981; Ohtsu and Ono 1984, 1986; Scruby 1985; Green 1995, 1998; Lysak 1996; Giordano et al. 1999; Wilcox et al. 2006).

As a common denominator in these theories, the dynamics of the AE source are inevitably linked to the dynamics of the crack growth. Hence, both the fractured material and the external loading determine the crack speed, which translate into a frequency bandwidth of the source. This results in characteristic frequency range for the AE signals between 10 kHz and 1 MHz observed for most materials, although the experimentally measured bandwidth is additionally compromised by the bandwidth of the type of sensor used.

The amount of energy released by an AE source event and the amplitude of the signal are related to the magnitude and also the velocity of the source event. As result from the basic theories above, the amplitude of the emission is expected to be proportional to the speed of crack propagation and the amount of surface area generated. Thus, large discrete crack jumps generate larger AE signals than those generated by cracks that propagate slowly over the same distance.

Another key characteristic of the AE source is the orientation and movement direction of the crack, which causes a distinct radiation pattern. For the typically thin structures used in aerospace applications, the position of the (microscopic) AE source in the thickness direction will additionally influence the excited frequency range since the originally undisturbed radiation pattern is turned into a guided acoustic wave.

However, material attenuation and guided wave dispersion effects will significantly affect the radiated frequencies and amplitudes as explained in Sect. 7.5. Therefore, numerous attempts have been published that provide analysis strategies for source identification considering the complexity of the situation faced.

7.3.1   AE Source Types

In the following, distinction is made for the established cases of AE source identification procedures for the types of defects categorised in Chap. 2.

For metallic materials, AE can result from the initiation and growth of cracks, particle fracture, sliding and dislocation movements, twinning or phase transformations (Grosse and Ohtsu 2008). Especially for aluminum, several researchers reported that particle fracture is one of the dominant sources for AE (Bianchetti et al. 1976; McBride et al. 1981; Cousland and Scala 1983; Wisner and Kontsos 2018; Wisner et al. 2019). For the fabrication of aircraft parts, typically thin metallic plates are applied, whereas reinforcement and joint elements can be associated with a more complex geometry. For the flat plate structures, substantial research was conducted to understand the relationship between source position, plate thickness and radiation direction. The use of numerical tools such as finite element modeling

provided huge insight in the way guided wave formation occurs in aluminum plates (Prosser et al. 1999; Hamstad et al. 2002a, 2002b; Hamstad 2010). This gave rise to the use of modal AE analysis and time frequency-based interpretation of AE signals as outlined in Sect. 7.3.2.

For composite materials, fracture may refer to the generation and propagation of cracks within the matrix material, along the matrix–fiber interface, or to the fracture of single fiber filaments or as a bundle. Another highly relevant source of AE found in fiber-reinforced polymers is the friction of existing crack surfaces. This occurs often during unloading and re-loading of damaged composites. Since many composites are laminates made from stacked layers with varying fiber orientations, the next scale for categorizing AE sources is the level of individual layers. When such laminates are loaded, cracks occur between the fibers, which grow parallel to the fiber orientation. Their dimensions are limited by the thickness of the layer (or the thickness of several layers when the fibers are oriented together). In addition, the stress concentration caused by such cracks as well as bending loads can induce delamination between the layers. During loading of a composite material or structure, all the mechanisms mentioned above may accumulate and interact until they ultimately cause a complete failure. AE is able to identify all these failure mechanisms, as it is sensitive to the multitude of different damage types spanning from the microscopic to the macroscopic scale (Sause 2016; Sause and Hamstad 2018). Meanwhile, this is not only supported by numerous experimental findings but now also by modelling approaches to predict the AE signal of a given source type, by analytical methods (Wilcox et al. 2006) and by finite element modelling (FEM) (Prosser et al. 1999; Sause and Horn 2010a, 2010b; Sause and Richler 2015). Therefore, considering the expected sequence of occurrence of the different fracture mechanisms, being able to identify the dominant one in real time offers information on the current structural condition and allows projections to the useful life span. As understood, fracture in composites is a fairly complicated and stochastic process because of several mechanisms as well as their possible overlap in time. This complexity is inevitably transferred to the AE signal making the interpretation less than straightforward. Still, some basic indicative principles can be mentioned as the starting point of the effort to understand the connection between AE signals and the original event. As Fig. 7.6 shows, a crack propagation event extending vertical to the axis of the plate results in waveform with different characteristics from a similar crack in the parallel direction. In the case of plates, the reason can be sought in the different amount of energy forming the 'symmetric' and 'antisymmetric' wave modes (Scholey et al. 2010; Eaton et al. 2011), depending on each case. When a vertical crack is extended (Fig. 7.6a top), this motion excites mostly symmetric components that have higher propagation velocities than antisymmetric, as already discussed in Chap. 5.2. A waveform containing stronger symmetric component is expected to have higher energy in the opening part rather than the later part; see example of Fig. 7.6b. By contrast, when a horizontal crack (delamination in the case of laminated plates) is extended (Fig. 7.6a bottom), the transient motion gives rise to the antisymmetric wave mode. Thus, it is reasonable that for the extreme cases of event orientation, differences are noticed in the waveform shape, practically
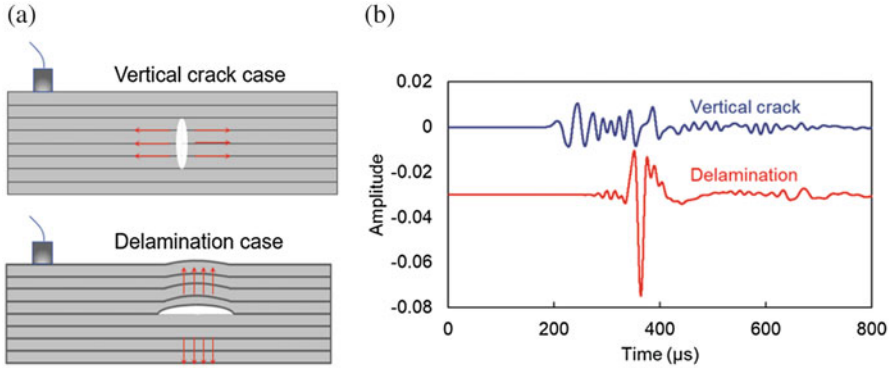
Fig. 7.6 (**a**) Representation of vertical crack (top) and delamination (bottom) in a laminated composite plate and (**b**) typical AE waveforms from the two events

resulting in shorter rise time for vertical cracks and longer durations for delaminations. Possible single fiber or fiber bundle rupture is expected to obtain even shorter duration characteristics and higher frequency content, as the fracture incident is usually shorter in time due to the limited fiber cross section to be fractured in one step and the higher speed of crack propagation within the high modulus fiber. The final waveform shape will be influenced by a number of aforementioned factors apart from the orientation, such as the position of the crack in the thickness (non-central sources will yield combination of modes instead of a single one), their displacement increment and speed and the propagation distance to the sensor and sensor characteristics as mentioned below. Despite the strongly stochastic nature of the processes, this visualization can be treated as a starting point of analysis, since it is supported by extended literature in the composites field (Sause and Hamstad 2018; Li et al. 2015; Blom et al. 2014; Kolanu and Raju 2019; Aggelis et al. 2012). Furthermore, recently AE has proven sensitive to the mode of the strain field (shear/tensile) before damage is inflicted in any measurable form (Kalteremidou et al. 2021).

In Fig. 7.7, the wavefields caused by a transverse crack and a delamination type source are contrasted. The source is assumed to happen at the same spot close to the hinge of a landing flap. The color scale is providing the out-of-plane velocity component of the guided waves excited in the airplane wings skin at two discrete time steps after crack growth. Based on the significantly different wavefields, it can readily be understood that the signals picked up by a sensor system will be significantly different as well. In addition, the different AE sources cause different guided wave modes as mentioned above, which will see different propagation behavior as described in Sect. 7.5.

For aircraft structures an additional item is the use of adhesives, coatings or interlayers combined with structural parts made from metals or composites. For the flat plate-like structures, they may be considered as an additional layer of different material that is attached or integrated with the plate. During the lifetime of the component, cracks may form inside the adhesive or coating or at the interface to the
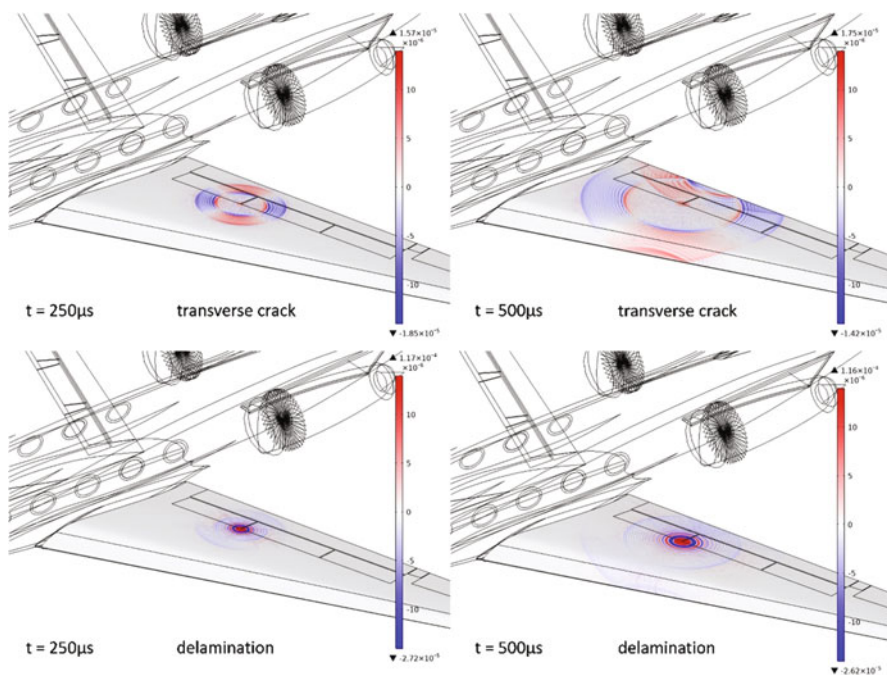
Fig. 7.7 Visualization of the out-of-plane velocity component of the wavefield emitted by a transverse crack (upper row) and delamination (bottom row) at two discrete time steps after the occurrence of the crack in aircraft wing skin.

structural material (Sause 2010). This sort of crack growth is expected to cause AE and was reported in literature several times (Piotrkowski et al. 2005; Sause et al. 2008; Sause et al. 2009; Yao et al. 2012).

7.3.2 Procedures for AE Source Identification

In the last twenty years, many approaches have been proposed that attempt to identify AE sources. These concepts include moment tensor inversion, time inversion approaches, guided wave analysis and pattern recognition techniques. When discussing these techniques, it is useful differentiating between signal classification and source identification. In signal classification, the task is to group signals based on similarity measures. Such clustering is often achieved by data analysis of multiple AE characteristics. The applied methods for AE signal clustering ranges from simple discrete feature value analysis to automated pattern recognition. After clustering of the AE signals, the task of source identification is to assign a specific cluster to a specific source type. Since all source identification procedures are based on the detected signal information it is essential that the AE sensor used does not inhibit the

recording of the required information. Therefore, if frequency information is desired as means of distinction of source types it is mandatory that the sensor covers enough bandwidth and does provide reasonable flatness to ensure proper detection of the propagating wave's frequencies.

Although, in volumetric media, the source type can be derived by moment tension inversion (Aki and Richards 1980; Ohtsu and Ono 1984; Grosse and Ohtsu 2008; Green 1995, 1998), this approach cannot be used in thin structures mainly because most of the information on the orientation of the source is lost in a few millimeters of propagation.

In recent years, the time reversal AE approach has been used to yield the (temporal) source function and the radiation behavior of the source (Ciampa and Meo 2010a; Ozevin and Heidary 2011; Ernst and Dual 2013). This has been demonstrated to measure the orientation of cracks in thin metal plates (Ozevin and Heidary 2011). Consequently, the time reversal approach could be used to obtain further information regarding the origin of the source. However, the approach faces the same challenge as moment tensor inversion, i.e. the precise knowledge of the Green's function of the propagation medium.

Another classification technique that is more suitable for composite materials is the analysis of guided waves. This approach uses the relationship between certain source types and their corresponding guided wave modes as occurring in in plate-like structures (Gorman 1991, 2011; Gorman and Prosser 1991; Gorman and Ziola 1991; Prosser et al. 1995, 1997; Prosser 1996; Morscher 1999; Surgeon and Wevers 1999). The aim is to find specific ratios of certain guided wave modes that are characteristic for a particular type of source. Although such ratios are partly expected, clear assignment of guided wave mode ratios to particular source mechanisms remains challenging. This whole procedure also requires the use of multi-resonant or broadband sensors to cover the frequency range of interest. Ideally, 'flat' sensors are used to avoid that additional resonance artifacts are superimposed on the signatures of the guided wave modes. As an example, it can be mentioned that in certain studies such as Martínez-Jequier et al. (2015), higher energy at low frequency content is associated to delamination events, whereas higher frequency content is associated either with matrix cracks in some cases or with fiber rupture. Practically, the above-mentioned processes are translated to different amplitude and frequency distributions for different failure mechanisms. Despite the general overlap that is stressed in all studies, in some of them, some general separation is suggested based on their amplitude or frequency content (Liu et al. 2012; Mahdavi et al. 2016; Chandarana et al. 2017; Li et al. 2014; Ramirez-Jimenez et al. 2004; De Groot et al. 1995; Li et al. 2014), where fiber breakage shows higher values than those of delaminations and even higher than those of matrix cracking. It is again highlighted, however, that although these processes are reasonably based on the physics of wave propagation in plates after specific source excitation and they are confirmed and used in several cases in literature, they exhibit stochastic character, and their validity for each separate AE event cannot be taken for granted and should be tested by secondary means such as post-mortem studies or validated modeling strategies.

In contrast to classical single AE feature analysis, pattern recognition techniques use a variety of AE features and can therefore be used to group different signal types. This helps to classify signals even when they cannot be distinguished by discrete feature limits, such as a particular peak frequency or particular signal amplitude. In principle, pattern recognition techniques can be divided into two branches, namely supervised pattern recognition and unsupervised pattern recognition. Some of the established pattern recognition approaches can be understood as more general classification routines that follow the idea of mode analysis of guided acoustic waves. Therefore, similar requirements apply to sensor technology (multi-resonant or broadband sensors).

In unsupervised pattern recognition the task is the separation of a set of given objects without prior knowledge into different groups based on their similarity relative to each other. Various approaches have been applied (Anastassopoulos and Philippidis 1995; Anastassopoulos et al. 1999; Baensch et al. 2015a, 2015b; De Oliveira et al. 2004; Doan et al. 2014; Huguet et al. 2002; Kostopoulos et al. 2003; Marec et al. 2008; Philippidis et al. 1998; Ramirez-Jimenez et al. 2004; Richardson et al. 1984; Sause and Horn 2010b; Sause et al. 2009; Sause et al. 2012; Vi-Tong and Gaillard 1987; Yu et al. 1996). As an alternative approach, supervised pattern recognition techniques comprise two successive stages. In the first stage, a set of objects with known assignments (so-called labels) is required. An algorithm is trained to establish a functional relationship between a given set of characteristics and their respective label. In the second stage, the algorithm is applied to objects with the same characteristics, but unknown labels. Based on the established functional relationship the algorithm then provides the object labels based on a measure of similarity to the training data. For this purpose, the distinction of noisy and non-noisy AE signals can be accomplished via unsupervised pattern recognition techniques (Anastassopoulos and Philippidis 1995; Philippidis et al. 1998). Acoustic emission signals resulting from friction and electromagnetic induction can be easily identified in this respect because of their inherent characteristic difference from transient acoustic emission signals (e.g. long constant amplitude signals with broad frequencies or short duration spikes). Through appropriate experimental considerations and finite element simulations, the respective signal types can also be associated with specific failure mechanisms (Bohse and Chen 2001; Haselbach and Lauke 2003; Huguet et al. 2002; Li et al. 2014; Li et al. 2015; Marec et al. 2008; Ramirez-Jimenez et al. 2004; Richardson et al. 1984; Sause and Horn 2010b; Sause et al. 2009; Sause et al. 2012).

Even though pattern recognition techniques are frequently used for AE signals, none of the approaches have yet made it to recognised standards. Meanwhile robust approaches for identification of natural clusters of AE signals have been proposed (Sause et al. 2012) and adopted for composites, wood fracture and study of plant dehydration (Njuhovic et al. 2014; Ritschel et al. 2014; Vergeynst et al. 2014a; Baensch et al. 2015b; Prieß et al. 2015). Influencing factors such as signal propagation, sensor type, pre-damaged material and geometry were identified (Sause and Horn 2010b; Sause 2013; Sause 2016; Sause et al. 2014). However, the main challenge still is the correct assignment of a group of signals to a corresponding

failure type. Therefore, the occurrence of natural clusters is worth considering, but is not sufficient for the correct labelling of the underlying AE source types. In addition, such labelling must be re-validated in each test configuration.

There are several established ways to perform such a task. One choice are phenomenological observations (Prosser et al. 1995), comparative measurements on specimens with known types of AE sources (Huguet et al. 2002; Scholey et al. 2010; Aggelis et al. 2012) or subsequent microscopy (Giordano et al. 1998; Kalteremidou et al. 2018) to verify the existence of damage types reaching to the surface level. X-ray micro computed tomography (μ-CT) has also been used to examine the damage within the volume of the components (Maillet et al. 2019; Zhou et al. 2021). However, these approaches have some drawbacks, as they require in-depth expertise and an understanding of the way signals propagate from the source to the sensor. The use of representative samples with model sources may also be misleading, because multiple microscopic AE sources may be generated at the same time instead of an intended single AE source.

Finally, modelling approaches have been used to allow the assignment of specific groups of signals to specific failure mechanisms, which allows to generate synthetic AE signals that can be subjected to the same feature extraction procedures as the experimental AE signals and then be compared (Sause and Horn 2010b; Burks and Kumosa 2014; Vergeynst et al. 2014b).

However, a general drawback of these AE source identification procedures is the assumption of a singular event happening isolated in time. In reality, damage formation may happen simultaneously and overlap in time. In addition, the time of occurrence of subsequent microscopic sources of damage may begin to overlap with the decay of earlier AE signals. This may lead to a 'continuous' stream of AE signals instead of single isolated signals for example when high loading rates are present. In case of such high AE activity, a clear distinction between different failure events is no longer feasible and partly renders source localization or source identification impossible.

Besides the AE sources from damage formation in the material, there are many other possible AE sources that might disturb the interpretation of damage-related AE. During the loading of a structure, there are inevitable physical connections to the surroundings. Oftentimes, the area of load introduction will be subject to stress-concentration effects, which results in preferential AE activity in that area. Since this additional AE activity can easily be detected by the AE sensors, it can easily be misunderstood as result of damage progression in the test section, although the material in the test section is barely damaged. The localization of AE sources can be helpful to reduce the recorded AE signals to those originating only from specific sections of the test structure. Moreover, structural supports are well-known to cause stick slip frictional movement between the support and the loaded structure. Stick-slip-friction is known to be a source that causes high AE activity. To reduce this contribution, a good practice is the use of lubricants at the supports to minimize the friction, or to apply source localization techniques to limit the interpretation on AE signals coming from other parts of the structure. It is also known that electrically driven machines or other powerful electronic devices may cause electromagnetic

induction in the sensor cabling, resulting in spike signals that are not resulting from any damage. In particular, changing the orientation of the cabling relative to the electric devices, as well as adequate grounding, can improve the situation and thus avoid such signals. Generally, the use of sensors with internal preamplifiers can reduce extraneous signals induced in cables, as the signal voltage level is raised directly behind the sensor, therefore resulting in a voltage level much less influenced by the induced noise floor. In addition, actuators or rotating components are subject to internal friction, which can also lead to the generation of artificial AE sources that are detected by the AE equipment. In particular, servo-hydraulic machines usually generate noticeable AE by operating the servo valve, which may interfere with proper detection of AE signals from crack formation. Unlike these artificial AE noise sources, audible noise or vibrations do not necessarily interfere with AE measurements, since these are often predominantly active in the audible range and below. Compared to that, AE measurements start above 10–20 kHz and typically extend to 1 MHz.

Regardless of the type of approach pursued, it is a key requirement to be able to detect the AE signals at all. Based on signal propagation effects (see Sect. 7.5), the signals may easily fall below the detection threshold. Even long before, the reduction of signal-to-noise ratio may lead to severe difficulties for proper source identification as the signal information is affected by digitization effects and coverage by the system electronics noise.

7.4 Localization

From aerospace point-of-view, AE-based inspection strategies are concerned with thin plates and large monitoring areas. This fact reduces the dimensionality of the problem, from 3D to 2D. Although the basic principle of localization is founded on the time difference of arrival (TDOA) measurement for different sensors, physics of wave propagation in plates make the acoustic source localization procedure (ASLP) quite complex. Frequency-dependent wave velocity (i.e. dispersion), multi-modal wavefield, mode-dependent amplitude characteristics make the ASLP difficult (see Chap. 5.2 for guided wave characteristics). Further complexity on the localization procedures may be imposed by direction-dependent properties of fiber-reinforced or woven plastic composites that are common in aerospace structures. Although in many practical cases composite plates are designed as orthotropic or transversally isotropic, non-uniform distribution of fibers or other design-specific features may result in substantial deviations from quasi-omnidirectional wave speed characteristics. Anisotropic elastic properties, resulting in different wave propagation velocities for different directions, bring severe complexity to source localization. Another consequence of anisotropy is difference between the direction of wave propagation, i.e. the wavevector $\mathbf{k}$, and the energy propagation direction (i.e. the group velocity vector, $\mathbf{V_g}$) due to non-circular constant-frequency contours of the dispersion relation (Wolfe 2005). Since localization techniques estimate direction of arrival of the

incident wave using different features of the waveform, e.g. local wavenumber, phase or amplitude correlation etc., it needs to be carefully analyzed whether the direction of $\mathbf{V_g}$ or $\mathbf{k}$ is found. For the former, those techniques are approximately valid for materials displaying small directional deviations between $\mathbf{k}$ and $\mathbf{V_g}$, and/or sources aligned with material symmetry planes—weakly anisotropic composites.

The inspection strategy adopted for ASLP also plays an important role for accuracy. Two main approaches for ASLP rely on periodic or continuous monitoring. In each case, different factors influencing the localization process need to be considered. Some of the factors include mounting and dismounting AE sensors to the structure and their repositioning contrasted to fixed and permanently mounted devices; temperature and time, i.e. aging factors (related to both the structure and the AE system elements), calibration and re-calibration, operator specific issues (e.g. mounting, coupling, calibration) and other. It is therefore of interest to employ ASLP techniques that will be possibly robust to the above factors. This can be (at least partially) achieved by using wave features displaying least possible sensitivity to system's conditions in a particular application, e.g. phase for systems in stable—and energy for unstable—environmental conditions.

This section aims at outlining most widely used ASLP techniques and discussing their capabilities in the context of the above-mentioned requirements. It should be noted that the methods listed in this section are selected from a wide variety of available techniques. Their application typically depends on a number of factors like the type and characteristics of the sensors, acquisition mode, accessibility to the structure hot-spots, time, desired accuracy, availability of material properties of the structure, its geometrical and material complexity, expected type of acoustic source (e.g. impact/crack or leakage) and others. One of important restrictions for a potential ASLP method is the number of sensors applied. A localization method should use minimum possible number of sensors due to: weight and service issues, redundancy and self-check/self-diagnostics and calibration should be possible within the network of sensors, robustness of the system to a single-sensor failure; amount of transferred/processed data etc.

The ASLP methods can be in general classified into two groups: localization with and without knowing material properties of the medium. Knowing material properties substantially simplifies and in general improves accuracy of localization. However, precise information on elastic properties of the medium is most frequently unknown, in particular in the case of anisotropic media. In fact, most of the methods of practical importance are applicable up to moderately anisotropic plates due to fact that for non-coincident $\mathbf{k}$ and $\mathbf{V_g}$, the direction of energy propagation does not point to the source in general. What is more, for isotropic media, those methods can be frequently applied directly and without the need for solving complex nonlinear equations. Approximate estimates of wave velocities may partially circumvent the problem, but impact localization accuracy. Consequently, methods that do not require material properties for finding the acoustic source location are appealing.

The classical state-of-the-art localization is based on the time difference of arrival (TDOA) measurement for a network of sensors. TDOA is computed from signals acquired by the sensors. During monitoring, all sensors simultaneously register

Fig. 7.8 Acoustic source
localization via triangulation
for known wave speed c
(after Kundu 2014)
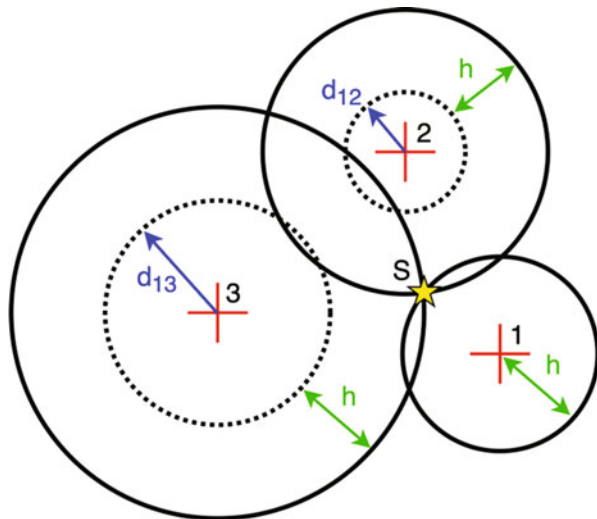
signals and store them in a circular buffer. The signals are continuously checked and
recording starts upon threshold crossing at any of the sensors. After registering an
AE event, the signals are analysed and localization estimates are computed by
dedicated algorithms, as discussed later. Threshold value depends on application,
type of sensor and coupling agent used and is typically adjusted by the operator. Too
low threshold value may result in registering invaluable data while too high—
missing AE events. Particular localization strategy depends on whether the wave
speed in the plate is known at least approximately or unknown—then the TDOA can
be combined with a simple iterative triangulation search (Tobias 1976) or a solution
of a set of nonlinear equations (frequently solved through an optimization) (Liang
et al. 2013). The method has been widely applied in laboratory and industrial
conditions, for isotropic and weakly anisotropic plates.

For a triangulation of an acoustic source when the wave speed, c, for an isotropic
plate is known, the following simple procedure can be followed (Tobias 1976;
Kundu 2014). A set of three sensors—1, 2 and 3, as shown in Figs. 7.8 and 7.9—
is placed non-collinearly on the plate. Acoustic source generates an elastic wave that
travels from point S (source location, denoted by the yellow star) to the sensors.
Although the moment of emission—hence the travel time—from the source is
unknown, the TDOA between the sensor that receives the event first (e.g. 1) and
the two remaining sensors (e.g. 2 and 3), e.g. T_{12} and T_{13}, are known. Consequently,
the distances travelled by the wave in that times are $d_{12,13} = c\,T_{12,13}$. Next, circles of
diameters d_{12} and d_{13} are drawn with sensors 2 and 3 in the centers, respectively
(circle at sensor 1 is of radius zero). Finally, to locate the source S, the radii of the
three circles are increased uniformly by h until they meet at a common point, as
shown in Fig. 7.8. It needs to be noted that the initial estimate of c is important for
localization and different values of wave velocity result in different predicted

Fig. 7.9 Acoustic source localization via triangulation for known wave speed 2c (after Kundu 2014)
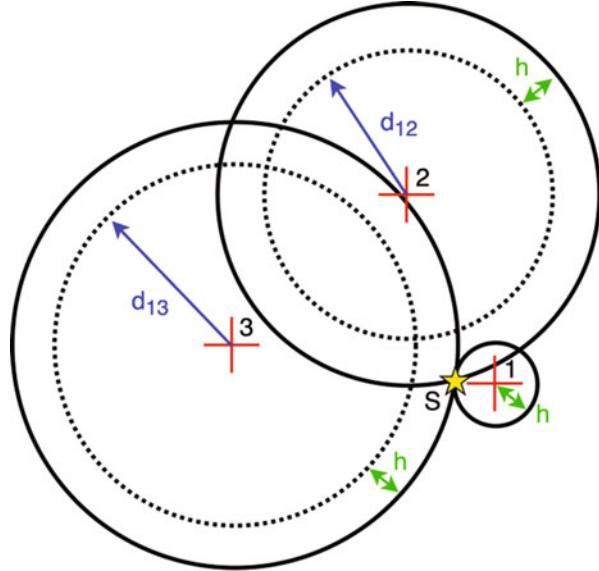
positions of S, as shown in Fig. 7.9. This ambiguity can be (at least partially) resolved by adding redundant sensors to the system.

The above-mentioned triangulation technique for ASLP can be re-formulated in order to avoid the requirement of knowing the wave velocity, c. In that case however, a set of nonlinear trigonometric equations need to be solved in order to locate the source (Liang et al. 2013).

ASLP techniques for plates that require the wave speed as an input parameter suffer additional accuracy problems due to multimodal and dispersive nature of Lamb waves that propagate in these structures. A single value of wave speed does not account for multiple wave modes and the fact that waves at different frequencies propagate at different speeds. Since AE signals are mostly broadband or narrow-, but finite, band, the dispersion effect plays a substantial role in ASLP in guiding media. A method combining the simplicity of the triangulation approach with basic information on wave physics in plates can be found in (Grabowski et al. 2016a). The method employs the time-distance domain transform (TDDT) for mapping the signals acquired by the sensors, transforming them from the time to the distance domain. Subsequently, the localization is performed immediately in the distance domain to find the acoustic source.

In the TDDT-based ASLP (Grabowski et al. 2016a) it is assumed that the source generates a signal whose Fourier transform is denoted by $S_{exc}(\omega)$. The signal travels through the plate and is acquired by the jth sensor as $S_{acq, j}(\omega)$. The propagation medium (i.e. the plate) transforms the excited signal into the acquired signal as follows

$$S_{(acq,j)}(\omega) = G(r_j, \omega) S_{exc}(\omega), G(r_j, \omega) = A(r_j, \omega) e^{-ik(\omega)r_j} \qquad (7.3)$$

where the signal deformation due to the acquiring sensor characteristics has been neglected (for a full derivation the reader is referred to (Grabowski et al. 2016a). In Eq. (7.3), G is the transfer function of the plate (assuming the far field propagation conditions), $A(r_j, \omega)$ is the frequency- and distance-dependent amplitude characteristic of the plate, $k(\omega)$ is the dispersion (phase) characteristic and r_j is the unknown distance between the source and the jth sensor. Clearly, the dispersion curves, $k(\omega)$, impose a phase shift for each frequency component of the excited signal.

When material properties and plate thickness are (at least approximately) known, then $k(\omega)$ can be computed and used for mapping the acquired signals from the time to the distance domain. The latter is possible through the sequence of mapping transforms: time-to-frequency ($t \rightarrow \omega$), frequency-to-wavenumber ($\omega \rightarrow k$), wavenumber-to-distance ($k \rightarrow r$). Therefore, the dispersion characteristics work as the TDDT map. Using $k(\omega)$, Eq. (7.3) can be rewritten as

$$S_{exc}\left(k^{-1}(\omega)\right) = S_{exc}(k) = A^{-1}\left(r_j, k^{-1}(\omega)\right) e^{ik(\omega)r_j} S_{acq,j}\left(k^{-1}(\omega)\right) \qquad (7.4)$$

In Eq. (7.4), all characteristics are presented as functions of the wavenumber **k**, e.g. $S_{exc}(k^{-1}(\omega)) = S_{exc}(k)$. The distance-domain dispersion-compensated source signal, $S_{exc}(r)$, can be therefore obtained by the inverse Fourier transform of $S_{exc}(k)$ and immediately used for ASLP. For this purpose, three circles of radii r_1, r_2 and r_3 are drawn around respective sensors, analogously to those presented in Fig. 7.8. The crossing point of the three circles, or the area left between them, is the acoustic source location estimate.

The radii r_1, r_2 and r_3 are unknowns of equations generated from Eq. (7.4). Therefore, direct inversion of Eq. (7.4) is not possible until r_j are known. Location of the source, given by r_j, is found by realizing that: (a) all acquired signals should be the same after the mapping procedure (namely, there is one source signal that has been deformed differently along different propagation paths r_j) and (b) the amplitude envelope of the compensated signal is at its maximum for the correct r_j values (or, equivalently, the width of the source wave packet is the shortest). By iteratively time shifting the acquired signals and processing by the proposed algorithm, r_j corresponding to the actual source-sensor distances can be found. An example of the shifting procedure used for determining r_j is shown in Fig. 7.10, where the compensated signal amplitude and wave packet width are presented. Clearly, both of these parameters assume their extreme values for the same (or very close) time shift (meaning the same distance). Dispersion-compensated signal after transformation to the distance domain—obtained by applying the procedure outlined above—is shown in Fig. 7.11, along with the waveform before signal processing is applied.

An interesting feature of the TDDT-based method is its ability to differentiate between Lamb wave modes in the signals acquired at the sensors. By selecting different mode-specific branches from the dispersion plot and mapping the same (multi-modal) signal, it may be noted that only parts of the signal corresponding to
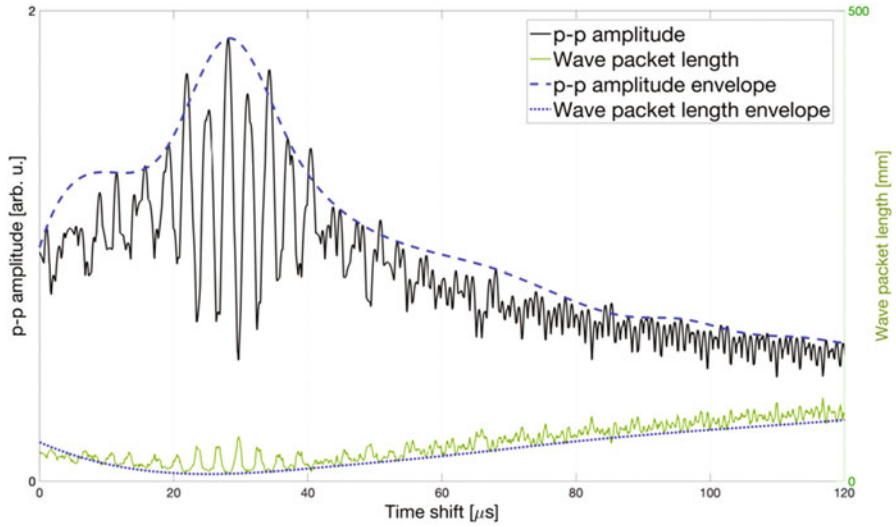
Fig. 7.10 Amplitude and width of a wave packet after dispersion compensation with various time shifts (after Gawronski et al. 2016)
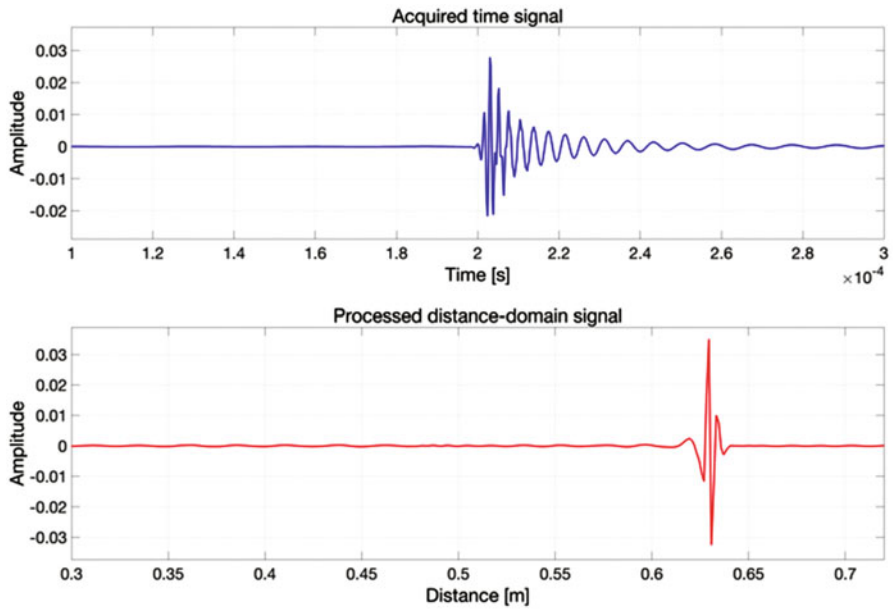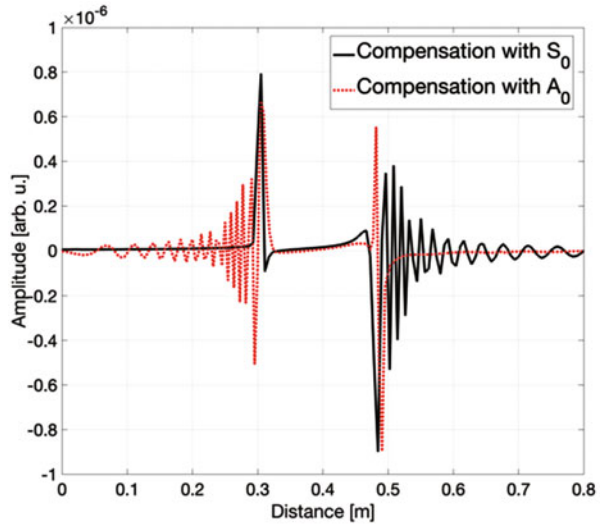

Fig. 7.11 Example signals: time-domain signal acquired at the source (top) and dispersion-compensated and transformed to the distance domain (bottom), after (Grabowski et al. 2016a)

Fig. 7.12 A dispersion-compensated signal mapped through dispersion branches for S_0 and A_0 modes

the mode that match the dispersion branch are properly compensated and placed at a correct distance. An example of such mapping is presented in Fig. 7.12 where the same time signal—containing the S_0 and A_0 wave packets—registered by a sensor was compensated by using the S_0 and (independently) A_0 mode characteristics (black and red lines, respectively). Each time the compensation is carried out only one of the wave packets is properly compressed, proving the ability of the method to distinguish between multiple wave modes.

It needs to be pointed out that the proposed mapping has important consequences and advantages for the localization process. First, the ASLP is performed in a natural, distance, coordinates. Second, no fixed assumption on a single wave velocity is made, but the full spectral characteristics of the medium are used. Therefore, any wave mode of arbitrary frequency band can be transformed. The effect of TDDT is compressive, i.e. the signal is dispersion-compensated and resembles the original signal shape at the source (pertaining to source identification). Finally, various wave modes can be selectively filtered by subsequent processing of the signals with different dispersion branches. As the above brief outline of the TDDT-based ALS neglects the impact of amplitude-frequency characteristics of the plate, the reader is referred to (Grabowski et al. 2016a, 2016b) for details.

In contrast to sparsely distributed sensors, a whole group of cluster-based localization techniques for plate-like structures is based on the concept of a group of three or more AE sensors (Kundu 2012), as shown in Fig. 7.13. The sensors forming a cluster need to be closely-spaced with respect to the distance to the source (D). In (Kundu 2012), a minimum of three sensors are arranged in a right-triangular setup (the so-called L-shaped cluster), however, other arrangements have also been developed, e.g. square (Sen et al. 2020), M-shaped (Grabowski et al. 2015) or Z-shaped (Yin et al. 2018). The concept of the cluster aims at immediately estimating the direction of incident wave knowing the sensors positions not material properties of
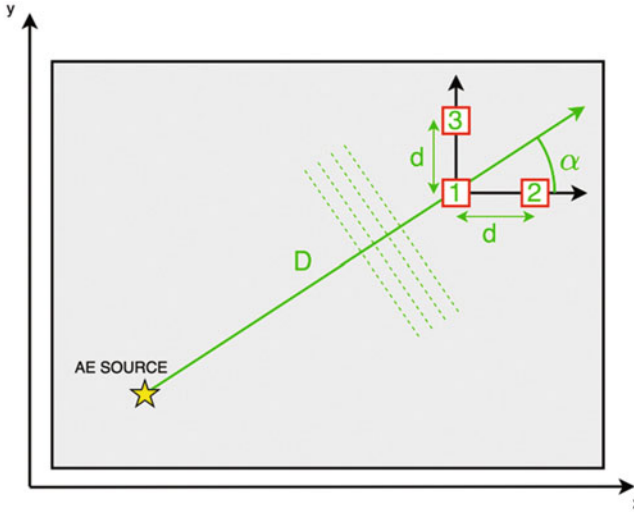
Fig. 7.13 A minimal cluster of three sensors required for estimation of direction of arrival (after Fig. 1 of Kundu 2012)

the medium. As shown in Fig. 7.13 for a single cluster, the incidence angle, α, for the source signal is estimated from two time delays of signals registered by the cluster, namely Δt_{12} and Δt_{13} (12 and 13 being the wave delays between sensors 1 and 2, and 1 and 3, respectively). Then, the angle is given as $\alpha = tan^{-1}(\Delta t_{13}/\Delta t_{12})$. It may be also noted that the two time delays allow for estimation of the group velocity along α direction, namely $V(\alpha) = d/\sqrt{\Delta t_{12}^2 + \Delta t_{13}^2}$. By using two clusters, two angles are found and the source is localised by solving two linear equations in two unknowns in a 2D space, as shown in Fig. 7.14. This procedure works for isotropic and weakly anisotropic materials, however, for the isotropic case only four sensors, i.e. a three-sensor cluster and a single additional sensor are sufficient for localization (Kundu 2012). In (Ciampa and Meo 2010a) also six sensors were used for ASLP on a composite plate, however, they were grouped in three clusters of two sensors each. This latter approach required the solution of a nonlinear set of equations. A hybrid approach based on the clusters and source location optimization was proposed in (Kundu et al. 2015), where the estimate of the source location is first is given by the technique outlined above (Kundu 2012), and this estimate is further improved by minimizing an error function.

Substantial difficulty with source location using incidence angle prediction may arise for moderately and strongly anisotropic materials. For certain wavefronts and cluster positions with respect to the source, the predicted angles may assume similar values, indicating that the source is very far from the sensing positions (or cannot be found when the predicted angles are equal, e.g. for a plane wave). A cluster-based solution for anisotropic materials, addressing the above issues, can be found in (Park
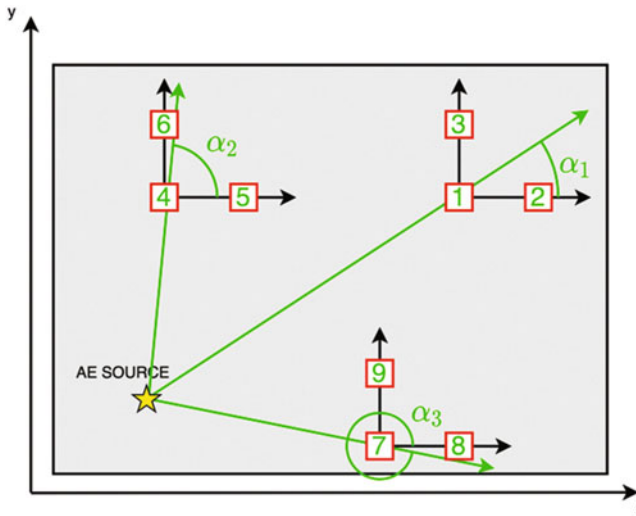
Fig. 7.14 A set of three clusters for (redundant) estimation of source localization (after Fig. 2 of Kundu 2012)

et al. 2017), where a set of three-sensor clusters was combined with an optimization procedure to locate the source. Knowing that for an anisotropic plate the wavefront assumes shapes different than circular, the proposed method assumes a parametric description of the wavefield emitted from the source and performs best fit for the model parameters using the arrival directions estimated by the clusters. In particular, two wavefront shapes—characteristic to weakly and moderately anisotropic plates— were assumed, i.e. elliptic and rhombus, respectively. The corresponding goal functions employ the ellipse and rhombus equations and include angles determined by the clusters. An example of an elliptic wavefront, requiring a minimum of three clusters is shown in Fig. 7.15, while for a rhombus wavefront—for which four clusters are needed—in Fig. 7.16.

Another approach to ASLP that uses collective response of possibly closely-spaced sensors, i.e. clusters, can be achieved by beamforming (McLaskey et al. 2010). Although beamforming (BF) techniques are widely known in active NDT and SHM, their application to acoustic emission is not that common. Acoustic source localization with beamforming employs the same signal processing techniques as in active methods and requires knowledge on material properties of the medium. Both isotropic (McLaskey et al. 2010) and anisotropic (Nakatani et al. 2012) structures can monitored with beamforming, if the wave speed profile—constant or angle-dependent, respectively—is known.

A method based on two perpendicular clusters of a total of 9 sensors and the beamforming algorithm for AE was proposed in (McLaskey et al. 2010; Xiao et al. 2014). The corresponding setup of ASLP with BF is shown in Fig. 7.17. Each of M sensors, placed at positions r_m, acquires signal $S_m(t)$ in case an AE event is generated. The cluster sweeps the two-dimensional space of possible acoustic source
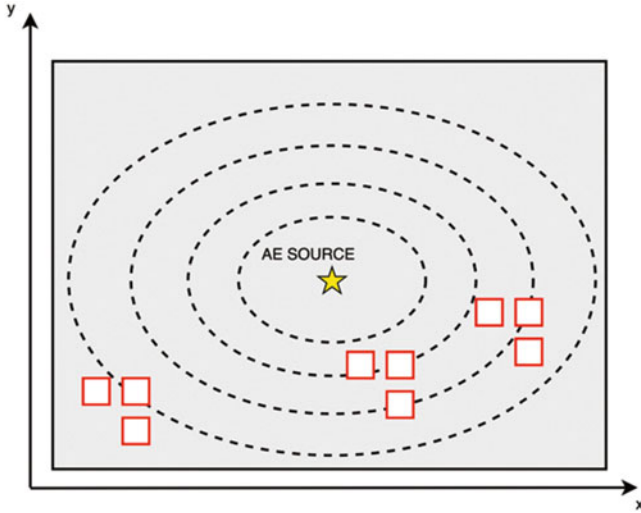
Fig. 7.15 Elliptic wavefront in an anisotropic plate with three clusters required for source localization (after Park et al. 2017)
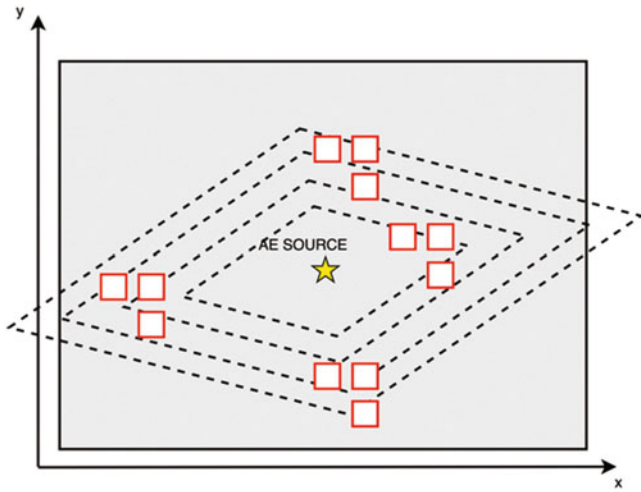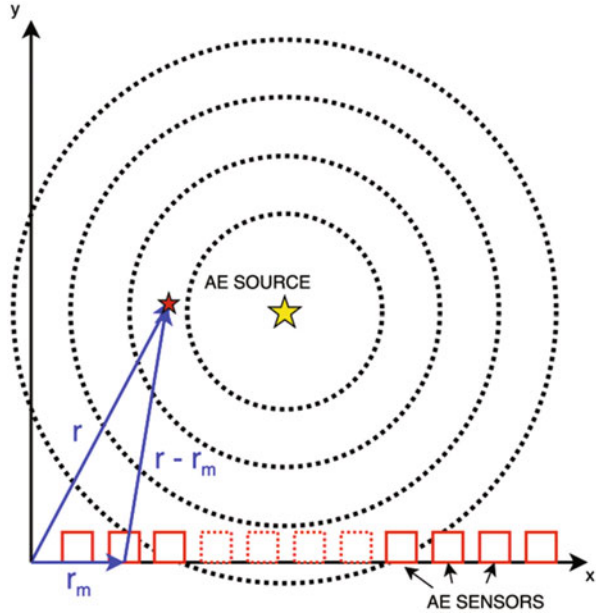

Fig. 7.16 Rhombus wavefront in an anisotropic plate with four clusters required for source localization (after Park et al. 2017)

locations (also known as focal points, red star in Fig. 7.17), r, by applying time delays

$$\Delta_m = \frac{(|r| - |r - r_m|)}{V} \tag{7.5}$$

to each of the S_m time signals and summing them

Fig. 7.17 Acoustic source localization with the beamforming approach (after Xiao et al. 2014)

$$b(r, t) = \frac{1}{M} \sum_{m=1}^{M} w_m S_m(t - \Delta_m) \qquad (7.6)$$

In Eq. (7.6), w_m are weights that can be applied to each individual sensor. $b(r, t)$ assumes maximum value if the focal point r coincides with the source position. In (Nakatani et al. 2012) this concept was further extended to anisotropic media by using direction-dependent wave speed $V(\alpha)$.

Clusters provide highly accurate localization results for isotropic and (weakly) anisotropic media, thus are of wide practical interest. The following factors, however, influence the cluster-based ASLP accuracy. (1) the distance between sensors, d, needs to be small, requiring small sensor footprints; (2) along with small d, the sampling frequency for the signals must be high enough to accurately capture waveform shifts between the sensors (i.e. accurate measurement of Δt); (3) the distance to the source, D, should be large compared to d, allowing for the planar wavefront approximation (and certain assumptions on incidence angles), (4) sensors need to be positioned very accurately within the cluster. Condition (3) implies the ability of monitoring large areas, however, with increasing D, the localization accuracy for anisotropic materials drops. The latter is a result of the non-colinear wave and energy propagation vectors.

To cope with AE localization problems with more sophisticated geometric structure, material/wave propagation characteristics, and flexible sensor configurations, AE localization can be formulated as an optimization problem, seeking a

solution (predicted source location) that leads to TDOA as consistent as possible with the measures. Such methods are mostly formulated as an iterative optimization process, starting from some initial guesses. Existing research proposed to use different optimization techniques. (Ciampa and Meo 2010b) uses Newton's method to optimise a nonlinear formulation to find the source location from an initial guess. Newton's method is known to converge quickly (with quadratic convergence) when the current estimate is close to the true solution. They further incorporate a line search strategy to optimise the step size to ensure improvement during iterations, to improve the robustness of the method. However, such local optimization methods may still converge to local minima. Alternative techniques have considered using more global optimization, such as genetic algorithms (Veloso et al. 2006), particle swarm optimization (Wang et al. 2017), an iterative evolutionary method named Iterative Planar Source method (Mirgal et al. 2020), etc. These methods typically start with a set of initial guesses (e.g. 50). For each estimated source location, they work out the calculated travel time to sensors, and the differences between calculated and measured travel times to sensors are used to calculate fitness values (or equivalent) of the estimated source location. These are then used to update sensor location estimations in the next iteration, with the exact formulae determined by the optimization techniques used. The iterative process tends to converge to a solution close to the true location. By using multiple estimated locations and iteratively optimizing them, such methods have a higher chance of finding the global optimum. More recent methods tend to converge more quickly than previous techniques.

These AE localization techniques still face challenges to cope with potentially complex reflections and reverberations of waveforms, and often ignore the rich signal content . In recent years, with the development of deep learning, techniques based on deep neural networks have been proposed as a way to tackle these challenges (Kalafat and Sause 2015; Ebrahimkhanlou and Salamone 2018a, 2018b). Thanks to the strong learning capabilities, deep neural networks often directly take some representations of the AE waveform as input, such as continuous wavelet transform to retain information in the rich waveform signal. Unlike many conventional techniques, typically based on using a single waveform feature, neural networks may exploit wider frequency bands—therefore richer signals. Different network architectures have been investigated, including an architecture that involves stacked autoencoder layers (which can be trained in an unsupervised manner to learn to extract useful features), followed by supervised layers to predict localization zones as a classification problem (Ebrahimkhanlou and Salamone 2018a) or regress the source location (Ebrahimkhanlou and Salamone 2018b). Alternative architectures such as those based on convolutional neural networks (CNNs) are also considered, where the waveform is analyzed with different times and frequencies to form an image-like input for the CNN to be applied (Ebrahimkhanlou and Salamone 2018a). Deep learning-based methods are able to utilise richer information in the waveform, which rather than being negatively impacted by reflections and reverberations, can effectively exploit such clues to help with localization. Studies

show that this can lead to more accurate localization (Kalafat and Sause 2015) or localization with fewer sensors including one sensor (Ebrahimkhanlou and Salamone 2018b), although sufficient amount of training data is required and more studies are needed for network architectures that reach a better balance of data demands and effectiveness of the learned models.

7.5   Influence of Propagation

A cracking source may be simulated by a near-step function or by half a cycle of short duration in case of impact, as studied in literature (McLaskey and Glaser 2012; Prosser 2002). However, this has no similarity to the much longer waveform recorded by a sensor just a few cm away, due to the complicated physics of wave propagation and transduction, see Fig. 7.18. The initial excitation (crack propagation increment or 'source' in our case) propagates through a material with certain characteristics (stiffness, density, attenuation coefficient, heterogeneity, as explained later in the chapter) which strongly influence its shape. Then at reception, the characteristics of the sensor, mainly frequency response will further influence the waveform (not forgetting the coupling conditions), while the acquisition system may also impose further distortion. Therefore, the final digitised waveform has very few similarities to the original source, see Fig. 7.18.

Making certain assumptions, like the point nature of the receiver, the final waveform (W) can be expressed as the convolution (*) between the initial excitation
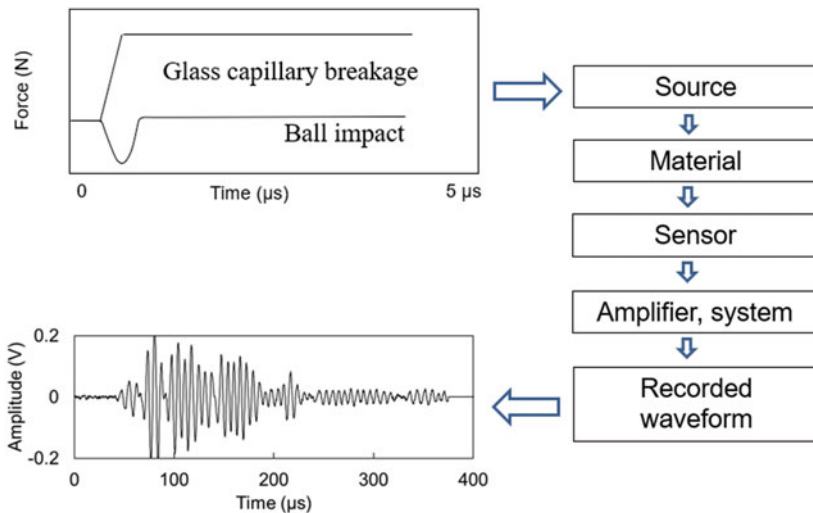

Fig. 7.18   Process chain of AE production and reception (Similar to McLaskey and Glaser 2012)

(E), and the transfer functions of the material (M), the sensor (S) and the amplifier/ system (A)

$$W = E * M * S * A \qquad (7.7)$$

This is easier handled in frequency domain, where the convolution is expressed by the product of the FFTs of the above functions.

Precise knowledge of the transfer functions of the material and system may allow therefore, to derive the source excitation using the waveform as received at the sensor, assuming that the sensor is not highly resonant. Still this is a tedious process and even slight mistakes in the included process links, may result in significant distortion at the end. Although, tracing back the exact source function may be difficult (though not impossible), still comparisons between sources can be readily conducted, if the experimental conditions remain the same (sensors, material, distance), that is all intermediate transfer functions are constant and therefore, they do not impose differential distortion between different signals.

Below follows a detailed discussion on the exact factors contributing to the above-mentioned material transfer function, which is also related to the Sect. 5.2 that described the formation and propagation mode of guided waves. There are several items that make the occurrence of guided waves unique in the context of AE measurements. Other than for active guided waves, AE sources cannot select a particular frequency or guided wave mode. Instead, based on the duration of crack growth they excite a certain bandwidth and—depending on the position in through-thickness direction—may excite one or more guided wave modes at the same time. Therefore, the interpretation of the AE signals has to deal with this additional complexity.

With the propagation of information in form of guided waves, several items happen. First, the whole wave undergoes attenuation, which can originate from several contributions. Secondly, the guided waves themselves suffer from information distortion due to dispersion. As consequence, after a certain propagation distance, the information contained in the AE signals will be altered, so that information retrieval about the source origin is only feasible up to a limited distance.

As discussed by Pollock (Pollock 1986) and Prosser (Prosser 1996) from the point of view of acoustic emission, there are five key contributions to attenuation:

1. Geometric spreading
2. Thermoelastic and Akhieser dissipation
3. Dispersion
4. Scattering
5. Dissipation into adjacent media

In the near-field range, close to the AE source, the geometrical spreading is the main reason for the attenuation. In volumetric media this is caused by the spherical radiation of energy into the volume, which leads to an energetic decay per dihedral angle with inverse propagation distance. For plate-like structures, the radiation is limited to two dimensions, after the 3D spreading in the very near field over the plate

thickness, causing an energetic decay with square-root of distance to the source. If such guided waves are excited, additional amplitude decay is present since the energy of the elastic waves is split into the distinct modes. In addition, these modes suffer from velocity dispersion, as described below.

In the far field of the AE source, the main contributions to the attenuation are due to thermoelastic and the Akhieser dissipation. The first results from the irreversible heat losses caused by compression during longitudinal wave propagation. The second mechanism results from the disturbance of the equilibrium distribution of the thermal acoustic waves (phonons), which leads to a dissipative energy contribution. In homogeneous isotropic solids, the thermoelastic and the Akhieser dissipation lead to an attenuation for elastic waves as a function of the square of the oscillation frequency.

In the case of guided waves, other effects contribute to the overall AE attenuation. In the case of Lamb waves, contributions to the total damping result from the spatial dispersion and the frequency dispersion (Neau et al. 2001). The attenuation from the spatial dispersion is caused by the relation between phase velocity and wave vector. As discussed by Ward et al. for dispersive media, the phase velocity is directly related to the attenuation by a Kramers-Kronig relationship (Ward 1971). The effect of attenuation due to frequency dispersion occurs during the propagation of non-monochromatic wave packages. Since each frequency component propagates at a certain velocity, an initially short pulse begins to spread in time during propagation. This causes an effective amplitude attenuation with distance of propagation. This is of great importance for the case of guided waves, since the different modes have different attenuation coefficients in addition. These effects are superimposed on the thermoelastic dissipation, since individual guided wave modes are dominated by distinct frequency portions (Prosser 1996). In addition, the propagating waves can be scattered by inhomogeneities depending on the wave frequencies and sizes of the inhomogeneities. Typical examples are the grain structure within metals, fibers in composites or cavities. This can lead to additionally strong attenuation and must be considered when discussing attenuation effects (Aggelis et al. 2004).

In real test settings or in SHM applications, AE signals propagate within the structure under test, which is typically in contact with adjacent items such as nearby structural parts, fittings, fasteners or supply lines. Since a partial transmission of the AE signal into adjacent media leads to a corresponding intensity loss of the reflected wave, such losses can be considerably high and thus even dominate the acoustic attenuation in a given scenario.

As a result of these propagation effects, the information contained in the amplitude and frequency of the AE signal formed during excitation is changed during propagation. Consequently, the detection and identification of a failure mechanism is limited to a certain distance around the position of the acoustic emission excitation. The influence of reflection should be mentioned as they contribute to the recorded signals and influence the obtained waveforms.

For fiber reinforced materials, the attenuation is typically much higher than for metallic materials. This increase of attenuation is due to the pronounced viscoelastic
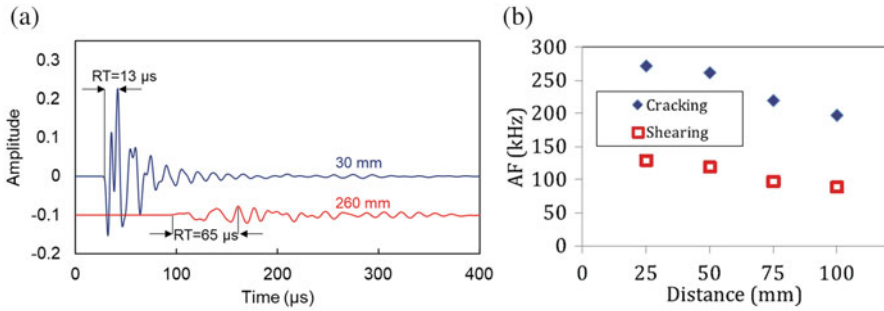
Fig. 7.19 (**a**) Simulated waveforms received at different distances from the source on a plate of 20 mm thickness, (**b**) average frequency, AF, for two fracture mechanisms vs. propagation distance in glass fiber composite (Aggelis et al. 2017)

response of the polymeric matrix materials, which are more prone to thermoelastic dissipation. Since higher frequencies are subject to higher attenuation, the relative loss of intensity can make it quite difficult for pattern recognition approaches to properly cluster AE signals of the same source type. Nevertheless, the attenuation effects can be investigated both experimentally and by FEM (Gallego and Ono 2012; Sause 2016) to consider their impact on AE signal interpretation.

In the following figure (Fig. 7.19a), an example of the influence of propagation on the waveform shape is shown. The simulations made through finite difference method concern a vertical crack propagation event in the middle of the thickness of a 20 mm thick plate of material with corresponding longitudinal wave velocity 3000 m/s. Despite the same origin, the two waveforms received at different spots exhibit strong differences in their shape. The amplitude of the second is significantly lower, while the aforementioned 'spreading' is obvious. Indicatively, the amplitude drops by 89% while the RT increases from 13 to 65 μs in just 230 mm of propagation. Fig. 7.19b shows an experimental example of such an effect, where the influence of distance on the average frequency 'AF' is shown for two major fracture mechanisms. Vertical cracking is connected to much higher frequency content for any corresponding distance than delaminations (shear), however, the decreasing trend is obvious due to aforementioned attenuation and dispersion mechanisms. It is seen therefore, that consideration of the distance (through localization) is of paramount importance, since signals emitted by high frequency sources but collected far away from the source, tend to obtain similar characteristics to signals coming from low energy sources but recorded close to the source (Aggelis et al. 2017).

7.6 Different Sensor Types

As thoroughly examined above, various physical phenomena in the material can cause elastic waves, which propagate throughout the material. The basic task of sensors is therefore, to detect surface displacements (typically out-of-plane) and to generate an electrical or optical signal. Piezoelectric sensors with an integrated element made of special ceramic, such as $Pb(Zr_xTi_{1-x})O_3$ or Lead Zirconate Titanate (PZT) are most often used in practice (Enoki et al. 2000; Moore 2005). PZT sensors need acoustic coupling for the dynamic surface motion of the specimen to result in dynamic strain in the piezoelectric transduction element which is reflected in voltage versus time signal. Piezoelectric transducers are most practical, they offer high sensitivity and are robust. PZT transducers are similar to PZT accelerometers except that the proof mass is replaced by a backing material to control damping. Resonant transducers that have one or more preferred frequencies of oscillation governed by crystal size and shape usually exhibit higher sensitivity and are less costly than broad-band piezoelectric transducers. The proper design of the PZT transducer offers a detection frequency range from 30 kHz to 1 MHz or in the case of resonant sensors, smaller frequency ranges. The transducers can have integrated preamplifier or the preamplifier is connected separately to the sensor. The amplified AE signal is transmitted via signal cables that can be of several hundred meters long to the AE system. Besides the mentioned advantages, they also have disadvantages, namely, the signal does not exactly resemble the actual surface displacements due to limited bandwidth, resonance, and are not always close to the point receiver concept, meaning that their response is the average field acting on their surface. This may cause serious distortion and attenuation when the wavelength is much smaller than the physical size of the transducer, especially for high frequencies (McLaskey and Glaser 2012; Ono 2017; Tsangouri and Aggelis 2018). PZT sensors are electrical sensors and therefore, are susceptible to electromagnetic interference, they also have a limited temperature range of operation (normal PZT cannot be used at temperatures more than 150 °C). In case high temperature application is necessary, the use of waveguides is essential (Godin et al. 2018; Papasalouros et al. 2016).

Recently, optical fiber systems have been gaining more importance for the detection of elastic waves in materials, thus directing research in the field of AE from electro-acoustic sensing technology to photoacoustic sensing technology. In general, optical fiber systems comprise optical sources that can be a laser, laser diode or light emitting diodes (LED), optical fibers, sensing element to transduce the measurement to an optical signal, an optical detector, and processing unit in a form of oscilloscope or optical analyzer. Based on the sensing location, an optical fiber sensor can be classified as extrinsic where the optical fiber is used to carry light to and from an external optical device for sensing or intrinsic where environmental perturbations influence the physical properties of the optical fiber. External perturbations can influence intensity, phase, frequency and polarization. In general, advantages of optical fiber sensors over conventional piezoelectric sensors are their relatively easier integration with little interference into a wide variety of

structures of different materials, immunity to electromagnetic interference, resistance to harsh environments, robustness, lightweight, multifunctional sensing capabilities such as strain, pressure, temperature and acoustic signals (Fidanboylu and Efendioglu 2009). Optical fiber sensors include single fiber and fiber device sensors, optical fiber interferometers, and fiber Bragg grating sensors (Wild and Hinckley 2008). There are many single fiber sensing methods for the detection of AE signals such as evanescent field coupler, fused tapered fiber coupler, frustrated total internal reflection, and fiber microbending. Several interferometer configurations have been proposed i.e. Michelson, Mach-Zehnder, Fabry-Perot, and Sagnac. Interferometric optical fiber sensors have limitation regarding gauge length of the sensor and consequent cross-sensitivity problems with other measurands such as static strain and temperature. Short length Fabry-Perot interferometers offer a significantly reduced gauge length. Shorter gauge lengths can be accomplished with various intensity based single fiber optical methods or with fiber Bragg grating sensors (Wild and Hinckley 2008). FBG sensors are small in size, can be embedded in the structure, and have high sensitivity that is directionally dependent and can affect its performance (Perez et al., 2006; Mabry et al. 2011; Wu and Okabe 2012).

Another type of contact acoustic emission sensor is the capacitive sensor. They constitute two separate electrodes where one electrode is fixed to the substrate. Electrodes are separated by a small gap and form a capacitor under a DC voltage bias. The vibration of the electrode produces a time-varying current. They have been successfully used in laboratory tests. Such transducers can have good fidelity where the electrical signal very closely follows the actual dynamic surface displacement, but typically minimum displacement measured is lower than with PZT sensors (Moore 2005). Capacitive sensors can be in the form of micro-electro-mechanical system (MEMS). MEMS-based transducers for AE can be small, and if produced on a large scale inexpensive. They can integrate several transducers with different resonant frequencies on the chip that covers the frequency range of interest(Ozevin et al. 2006). Ozevin reported almost three times lower signal to noise ratio in the dB scale for MEMS transducers compared to conventional PZT transducer with results in fewer AE events detected.

Contact transducers for AE measurements have disadvantages in monitoring AE behavior in small or thin specimens related with the size of the transducer. Non-contact optical transducers in a form of laser interferometry offer quantitative and highly localized measurements of the surface motion. They do not disturb elastic waves, also they are not limited by frequency response (Kline et al. 1978). Out-of-plane displacement and velocity of the surface movement can be measured. The laser beam can be focused at a very small spot of the order of microns. For higher sensitivity a reflective surface is needed and it is difficult to get an adequate signal to noise ratio (Enoki et al. 2000). The interferometer can be internally calibrated to yield absolute displacement amplitudes.

7.7   Dedicated Aeronautics Applications and Examples

Over the last 30 years AE monitoring has been used to assess damage initiation and growth in aircraft structures, primarily during ground testing (Martin et al. 1995). Within this early testing, problems arose regarding the quantity of data produced, distinguishing noise from damage, and accurate source localization in complex structures. In recent years the increasing use of carbon fibre reinforced polymers (CFRP) has introduced new challenges, in addition to those already faced. Recent developments have enabled more success with the technology in real applications. Although there are only limited cases of AE monitoring being used for in service structures, ground-based testing has been improved greatly by these advances. Haile et al. (2017) used 12 AE sensors to monitor four high risk areas during fatigue testing of a full-scale UH-60 helicopter fuselage. The composite fuselage was manufactured from advanced thermoplastics and thermoset carbon-fibre, with additional stiffeners. Time of arrival (TOA) was used to locate sources, however, complicity made this difficult. The work concluded that further methods were required to enable large-scale monitoring of complex structures in real operating conditions. A technique applied to aircraft structures to improve AE localization is the Delta-T approach. Initially developed by Baxter (Baxter et al. 2007) the technique requires the structure to be mapped with Hsu-Nielsen sources. From this, a map of the difference in arrival times at each pair of sensors can be created. Pearson et al. (2017) trialled the technique on a relatively simple A320 wing rib, where an average 9.3 mm increased accuracy was seen. Fatigue testing of an aluminium panel with a number of large holes was also presented. In this testing the Delta-T technique located AE events generated from a crack with greater accuracy, increased confidence and a greater number of lower energy events which were unsuccessful with the standard TOA technique. The technique was also used for location of damage on an A320 landing gear fatigue test, where a crack was located to 10 mm accuracy (Holford et al. 2017). In the early days of AE monitoring, only the amplitude and other simple features of the event were considered; this enabled noise filtering, however was very reliant on the skill of the engineer (Martin et al. 1995). As aforementioned, recent advances in classification, through approaches such as artificial neural networks ANN, enable automatic classification of waveforms, which enables clear differentiation between damage and noise (Crivelli et al. 2014).

Impact monitoring in aircraft structures is vital, in particular within carbon fibre reinforced polymers (CFRP) where barely visible impact damage (BVID) result in delamination of fibres, causing the strength of the structure to be compromised. Traditional non-destructive testing (NDT), required technicians to manually inspect the structure using ultrasonic probes, a time-consuming process that requires downtime for the aircraft. As existence of damage is inevitable, aircrafts are designed damage tolerant (Talreja and Phan 2019), increasing their weight. AE can be used to detect impact to an aircraft structure, either by detecting the impact itself, or any growth under fatigue. After the loss of space shuttle Columbia due to impact damage Prosser (Prosser et al. 2004) investigated the use of AE monitoring of the leading

edge of space shuttles. It was found that although accelerometers could locate impact events, ultrasonic sensors had lower background noise and so were more suited for impact detection. The detection of impact in a composite aircraft is not only vital during service, but also during manufacturing, where tools drop and knocks during transport cause damage. The earlier damage is detected, the quicker itis resolved, saving money. To detect impact during manufacture, wireless systems have been utilised, as the associated problems with battery life are less vital. Giannì et al. (2020) developed a low power system, capable of accurately determining the time of arrival of an impact wave at a piezoelectric sensor. The distributed array of sensor nodes were time correlated via GPS, and source localization performed at a central hub. Within this work impact sources were located on a simple aluminium plate, however advanced localization algorithms, such as the Delta-T method could be used.

In another application, the integrity of bearings within a helicopters main gearbox is vital, as the large speed reduction causes high forces, which make them prone to pitting, spalling and contact wear. SHM of these has been applied since the 1990s, known as Health and Usage Monitoring Systems (HUMS), which record and analyse vibrations. Although these systems have reduced accidents, they are not completely accurate, and failures still occur. This failure is generally attributed to the noise produced within the system masking the useful signals. In recent years AE has been applied to the problem, since the frequency of interest is higher than that generated by sliding and friction in the bearing. This has been shown to enable AE monitoring to identify the presence of damage significantly earlier than vibration techniques (Elasha et al. 2018).

7.8   General Considerations

While the use of SHM systems is imperative in an aerospace structure, several points should be examined to make sure the system works properly, and it is compatible with in-flight requirements. One is the additional weight the SHM system will bring, something that eventually accounts for higher fuel consumption and air transport cost. The potential weight saving of removing non-essential wiring from an aircraft could save an estimated 14–60 million over a commercial aircrafts life (Gao et al. 2018). Doing so would reduce costly and time-consuming maintenance and installation of wiring (Yedavalli and Belapurkar 2011). Commercially available wireless AE systems with transmission capacity of several hits/s exist (Mistras 2013; Shen 2017). However, while wireless systems are promising, they still require power. Batteries could supply the required energy, but are heavy, expensive and their performance is low in cold conditions typical of a flying aircraft, while their use is restricted in aerospace industry. Therefore, energy harvesting is a requirement combined with an energy storage device, such as a super capacitor. Vibrational harvesters and thermal-electric generators show potential, however, there is currently a gap between the generated and the required energy. Another issue of an in-flight SHM system is the generation of large amount of data, that could easily

reach rates of tens of MB/hour/channel. Transmission of such large amounts of data and especially full waveforms would be costly and power consuming (Anastasi et al. 2009). Therefore, intelligent processing and data management is needed to filter out non-essential data, something that would require integration of improved algorithms for damage localization and characterization into the hardware. Finally, another important point is the harsh environments that the wireless SHM system should operate in, meaning that any devise on board must pass a series of tests ranging from temperature to vibration-based testing. Only combination and optimization of all above aspects will enable unlocking the potential the true potential of a SHM system, while the specific issues are dealt with in more detail in the respective chapters.

References

Aggelis DG, Tsinopoulos SV, Polyzos D (2004) An iterative effective medium approximation (IEMA) for wave dispersion and attenuation predictions in particulate composites, suspensions and emulsions. J Acoust Soc Am 116:3443–3452. https://doi.org/10.1121/1.1810273

Aggelis DG, Barkoula N-M, Matikas TE et al (2012) Acoustic structural health monitoring of composite materials: damage identification and evaluation in cross ply laminates using acoustic emission and ultrasonics. Compos Sci Technol 72:1127–1133. https://doi.org/10.1016/j.compscitech.2011.10.011

Aggelis DG, Dassios KG, Kordatos EZ et al (2013) Damage accumulation in cyclically-loaded glass-ceramic matrix composites monitored by acoustic emission, the scientific world. 869467.

Aggelis DG, El Kadi M, Tysmans T et al (2017) Effect of propagation distance on acoustic emission fracture mode classification in textile reinforced cement. Constr Build Mater 152:872–879. https://doi.org/10.1016/j.conbuildmat.2017.06.166

Aki K, Richards PG (1980) Quantitative seismology, theory and methods. University Science Books, Sausalito

Anastasi G, Conti M, Di Francesco M, Passarella A (2009) Energy conservation in wireless sensor networks: a survey. Ad Hoc Netw 7:537–568

Anastassopoulos AA, Philippidis TP (1995) Clustering methodology for the evaluation of acoustic emission from composites. J Acoust Emission 13:11–21

Anastassopoulos AA, Nikolaidis VN, Philippidis TP (1999) A comparative study of pattern recognition algorithms for classification of ultrasonic signals. Neural Comput Appl 8:53–66. https://doi.org/10.1007/s005210050007

Baensch F, Sause MGR, Brunner AJ et al (2015a) Damage evolution in wood – pattern recognition based on acoustic emission (AE) frequency spectra. Holzforschung 69:357–365. https://doi.org/10.1515/hf-2014-0072

Baensch F et al (2015b) Damage evolution in wood – pattern recognition based on acoustic emission (AE) frequency spectra. Holzforschung 69(3):1–9. https://doi.org/10.1515/hf-2014-0072

Baxter MG, Pullin R, Holford KM et al (2007) Delta T source location for acoustic emission. Mech Syst Signal Process 21:1512–1520. https://doi.org/10.1016/j.ymssp.2006.05.003

Bendat JS, Piersol AG (1993) Engineering applications of correlation and spectral analysis, 2nd edn. Wiley, New York

Bianchetti R, Hamstad MA, Mukherjee AK (1976) Origin of burst-type acoustic emission in unflawed 7075-T6 aluminum. J Test Eval 4:313. https://doi.org/10.1520/JTE10518J

Blom J, El Kadi M, Wastiels J et al (2014) Bending fracture of textile reinforced cement laminates monitored by acoustic emission: influence of aspect ratio. Constr Build Mater 70:370–378. https://doi.org/10.1016/j.conbuildmat.2014.07.080

Bohse J, Chen J (2001) Acoustic emission examination of mode I, mode II and mixed-mode I/II interlaminar fracture of unidirectional fiber-reinforced polymers. J Acoust Emission 19:1–10

Burks B, Kumosa M (2014) A modal acoustic emission signal classification scheme derived from finite element simulation. Int J Damage Mech 23:43–62. https://doi.org/10.1177/1056789513484620

Chandarana N, Sanchez DM, Soutis C et al (2017) Early damage detection in composites during fabrication and mechanical testing. Materials 10:685. https://doi.org/10.3390/ma10070685

Ciampa F, Meo M (2010a) A new algorithm for acoustic emission localization and flexural group velocity determination in anisotropic structures. Compos A 41:1777–1786. https://doi.org/10.1016/j.compositesa.2010.08.013

Ciampa F, Meo M (2010b) Acoustic emission source localization and velocity determination of the fundamental mode A0 using wavelet analysis and a Newton-based optimization technique. Smart Mater Struct 19. https://doi.org/10.1088/0964-1726/19/4/045027

Cousland SMK, Scala CM (1983) Acoustic emission during the plastic deformation of aluminium alloys 2024 and 2124. Mater Sci Eng 57:23–29. https://doi.org/10.1016/0025-5416(83)90023-X

Crivelli D, Guagliano M, Monici A (2014) Development of an artificial neural network processing technique for the analysis of damage evolution in pultruded composites with acoustic emission. Compos Part B Eng 56:948–959. https://doi.org/10.1016/j.compositesb.2013.09.005

De Groot PJ, Wijnen PAM, Janssen RBF (1995) Real-time frequency determination of acoustic emission for different fracture mechanisms in carbon/epoxy composites. Compos Sci Technol 55:405–412. https://doi.org/10.1016/0266-3538(95)00121-2

De Oliveira R, Frazão O, Santos JL et al (2004) Optic fibre sensor for real-time damage detection in smart composite. Comput Struct 82:1315–1321. https://doi.org/10.1016/j.compstruc.2004.03.028

Doan DD et al. (2014) Application of an unsupervised pattern recognition approach for AE data originating from fatigue tests on CFRP. In: 31st Conference of the European working group on acoustic emission. Dresden, Germany, pp 1–8.

Eaton M, May M, Featherston C et al (2011) Characterisation of damage in composite structures using acoustic emission. J Phys Conf Ser 305:012086. https://doi.org/10.1088/1742-6596/305/1/012086

Ebrahimkhanlou A, Salamone S (2018a) Single-sensor acoustic emission source localization in plate-like structures using deep learning. Aerospace 5:50. https://doi.org/10.3390/aerospace5020050

Ebrahimkhanlou A, Salamone S (2018b) Single-sensor acoustic emission source localization in plate-like structures: a deep learning approach. In: Proceedings of the Volume 10600, health monitoring of structural and biological systems, XII. http://www.ncbi.nlm.nih.gov/pubmed/106001O.

Elasha F, Greaves M, Mba D (2018) Planetary bearing defect detection in a commercial helicopter main gearbox with vibration and acoustic emission. Struct Heal Monit 17:1192–1212. https://doi.org/10.1177/1475921717738713

Enoki M, Watanabe M, Chivavibul P et al (2000) Non-contact measurement of acoustic emission in materials by laser interferometry. Sci Technol Adv Mater 1:157–165. https://doi.org/10.1016/S1468-6996(00)00017-6

Ernst R, Dual J (2013) Acoustic emission source detection using the time reversal principle on dispersive waves in beams. In: Proceedings of the 2013 international congress on ultrasonics (ICU 2013). Singapore, pp 87–92. http://www.zfm.ethz.ch/pdf/13-Ernst-1.pdf

Esola S, Wisner BJ, Vanniamparambil PA et al (2018) Part qualification methodology for composite aircraft components using acoustic emission monitoring. Appl Sci 8:1490. https://doi.org/10.3390/app8091490

Fidanboylu K, Efendioglu HS (2009) Fiber optic sensor and their applications. In: 5th International advanced technologies symposium (IATS'09), May 13-15. Karabuk, Turkey

Fowler TJ (1977) Acoustic emission testing of fiber reinforced plastics. ASCE Fall Convention, San Francisco

Gallego A, Ono K (2012) An improved acousto-ultrasonic scheme with lamb wave mode separation and damping factor in CFRP plates. J Acoust Emission 2012:109–123

Gao S, Dai X, Hang Y, Guo Y, Ji Q (2018) Airborne wireless sensor networks for airplane monitoring system. Wireless Commun Mobile Comput 2018. https://doi.org/10.1155/2018/6025825

Gawronski M, Grabowski K, Russek P et al (2016) Acoustic emission source localization based on distance domain signal representation. Proc SPIE 9805 Health Monit Struct Biol Syst 2016:98050I.

Giannì C, Balsi M, Esposito S et al (2020) Low-power global navigation satellite system-enabled wireless sensor network for acoustic emission localisation in aerospace components. Struct Control Heal Monit 27:1–13. https://doi.org/10.1002/stc.2525

Giordano M, Calabro A, Esposito C et al (1998) An acoustic-emission characterization of the failure modes in polymer-composite materials. Compos Sci Technol 58:1923–1928. https://doi.org/10.1016/S0266-3538(98)00013-X

Giordano M, Condelli L, Nicolais L (1999) Acoustic emission wave propagation in a viscoelastic plate. Compos Sci Technol 59:1735–1743. https://doi.org/10.1016/S0266-3538(99)00035-4

Godin N, Reynaud P, Fantozzi G (2018) Challenges and limitations in the identification of acoustic emission signature of damage mechanisms in composites materials. Appl Sci 8:article number 1267. https://doi.org/10.3390/app8081267

Gorman MR (1991) Plate wave acoustic emission. J Acoust Soc Am 90:358–364. https://doi.org/10.1121/1.401258

Gorman MR (2011) Modal AE analysis of fracture and failure in composite materials, and the quality and life of high pressure composite pressure cylinders. J Acoust Emission 29:1–28

Gorman MR, Prosser WH (1991) AE source orientation by plate wave analysis. J Acoust Emission 9:283–288. https://calhoun.nps.edu/handle/10945/40334

Gorman MR, Ziola SM (1991) Plate waves produced by transverse matrix cracking. Ultrasonics 29:245–251. https://doi.org/10.1016/0041-624X(91)90063-E

Grabowski K, Nakatani H, Gawronski M et al (2015) System reliability for verification and implementation. In: Proceedings of the 10th international workshop on structural health monitoring optimization of acoustic source localization in large plates. IWSHM 2015.

Grabowski K, Gawronski M, Baran I et al (2016a) Time–distance domain transformation for acoustic emission source localization in thin metallic plates. Ultrasonics 68:142–149. ISSN 0041-624X

Grabowski K, Gawronski M, Staszewski WJ et al (2016b) Acoustic emission source localization through excitability prediction and dispersion removal technique. IIIAE, Kyoto, p IAES-23 & ICAE-8, Kyoto, Japan

Green ER (1995) Acoustic emission sources in a cross-ply laminated plate. Compos Eng 5:1453–1469. https://doi.org/10.1016/0961-9526(94)00072-H

Green ER (1998) Acoustic emission in composite laminates. J Nondestruct Eval 17:117–127

Grosse CU, Linzer LM (2008) Ch. 5 Signal-based AE analysis, In:, Grosse CU, Ohtsu M (ed) Acoustic emission testing, pp 53-99.

Grosse CU, Ohtsu M (2008) Acoustic emission testing. Springer, Berlin Heidelberg. https://doi.org/10.1007/978-3-540-69972-9

Haile MA, Bordick NE, Riddick JC (2017) Distributed acoustic emission sensing for large complex air structures. Struct Heal Monit 17:624–634. https://doi.org/10.1177/1475921717714614

Hamstad MA (1986) A discussion of the basic understanding of the Felicity effect in fiber composites. J Acoust Emission 5:95–102

Hamstad MA (2010) Frequencies and amplitudes of AE signals in a plate as a function of source rise time. In: 29th European conference on acoustic emission testing. Vienna, Austria, pp 1–8.

Hamstad MA, O'Gallagher A, Gary J (2002a) A wavelet transform applied to acoustic emission signals: part 1: source identification. J Acoust Emission 20:39–61

Hamstad MA, O'Gallagher A, Gary J (2002b) A wavelet transform applied to acoustic emission signals: part 2: source location. J Acoust Emission 20:62–82

Haselbach W, Lauke B (2003) Acoustic emission of debonding between fibre and matrix to evaluate local adhesion. Compos Sci Technol 63:2155–2162. https://doi.org/10.1016/S0266-3538(03)00193-3

Holford KM, Eaton MJ, Hensman JJ et al (2017) A new methodology for automating acoustic emission detection of metallic fatigue fractures in highly demanding aerospace environments: an overview. Prog Aerosp Sci 90:1–11. https://doi.org/10.1016/j.paerosci.2016.11.003

Huguet S, Godin N, Gaertner R et al (2002) Use of acoustic emission to identify damage modes in glass fibre reinforced polyester. Compos Sci Technol 62:1433–1444. https://doi.org/10.1016/S0266-3538(02)00087-8

Kaiser J (1950) Untersuchung über das Auftreten von Geräuschen beim Zugversuch, PhD Thesis, Technische Hochschule Munich

Kalafat S, Sause MG, GR (2015) Acoustic emission source localization by artificial neural networks. Struct Health Monit 14:633–647. https://doi.org/10.1177/1475921715607408.

Kalteremidou K-A, Aggelis DG, Hemelrijck DV, Pyl L (2021) On the use of acoustic emission to identify the dominant stress/strain component in carbon/epoxy composite materials. Mechanics Research Communications, 111, art. no. 103663.

Kalteremidou K-A, Murray BR, Tsangouri E et al (2018) Multiaxial damage characterization of carbon/epoxy angle-ply laminates under static tension by combining in situ microscopy with acoustic emission. Appl Sci 8. https://doi.org/10.3390/app8112021

Kline RA, Green RE, Harvey Palmer CH (1978) A comparison of optically and piezoelectrically sensed acoustic emission signals. J Acoust Soc Am 64:1633–1639. https://doi.org/10.1121/1.382129

Kolanu NR, Raju G, M R (2019) Damage assessment studies in CFRP composite laminate with cut-out subjected to in-plane shear loading. Compos Part B Eng 166:257-271. doi:https://doi.org/10.1016/j.compositesb.2018.11.142.

Kostopoulos V, Loutas TH, Kontsos A et al (2003) On the identification of the failure mechanisms in oxide/oxide composites using acoustic emission. NDT E Int 36:571–580. https://doi.org/10.1016/S0963-8695(03)00068-9

Kundu T (2012) A new technique for acoustic source localization in an anisotropic plate without knowing its material properties, In: 6th European workshop on structural health monitoring, Dresden, Germany, July 3–6 2012

Kundu T (2014) Acoustic source localization. Ultrasonics 54:25–38ISSN 0041-624X. https://doi.org/10.1016/j.ultras.2013.06.009

Kundu T, Yang X, Nakatani H et al (2015) A two-step hybrid technique for accurately localizing acoustic source in anisotropic structures without knowing their material properties. Ultrasonics 56:271–278. https://doi.org/10.1016/j.ultras.2014.08.009

Li L, Lomov SV, Yan X et al (2014) Cluster analysis of acoustic emission signals for 2D and 3D woven glass/epoxy composites. Compos Struct 116:286–299. https://doi.org/10.1016/j.compstruct.2014.05.023

Li L, Lomov SV, Yan X (2015) Correlation of acoustic emission with optically observed damage in a glass/epoxy woven laminate under tensile loading. Compos Struct 123:45–53. https://doi.org/10.1016/j.compstruct.2014.12.029

Liang D, Yuan S, Liu M (2013) Distributed coordination algorithm for impact location of preciseness and real-time on composite structures. Measurement 46:527–536. https://doi.org/10.1016/j.measurement.2012.08.011

Liu PF, Chu JK, Liu YL et al (2012) A study on the failure mechanisms of carbon fiber/epoxy composite laminates using acoustic emission. Mater Des 37:228–235. https://doi.org/10.1016/j.matdes.2011.12.015

Lysak MV (1996) Development of the theory of acoustic emission by propagating cracks in terms of fracture mechanics. Eng Fract Mech 55:443–452. https://doi.org/10.1016/0013-7944(96)00026-4

Mabry N, Banks C, Toutanji H et al. (2011) Acoustic emission felicity ratio measurements in carbon composites laminates using fiber Bragg grating sensors. In: Proc SPIE. Singapore-M.I.T alliance for research and technology center, Sens. Phenom. Technol. Netw. Syst. 7982

Mahdavi HR, Rahimi GH, Farrokhabadi A (2016) Failure analysis of $(\pm 55°)_9$ filament-wound GRE pipes using acoustic emission technique. Eng Fail Anal 62:178–187. https://doi.org/10.1016/j.engfailanal.2015.12.004

Maillet E, Singhal A, Hilmas A, Gao Y, Zhou Y, Henson G, Wilson G (2019) Combining in-situ synchrotron X-ray microtomography and acoustic emission to characterize damage evolution in ceramic matrix composites. J Eur Ceramic Soc 39(13):3546–3556. https://doi.org/10.1016/j.jeurceramsoc.2019.05.027

Marec A, Thomas J-H, El Guerjouma R (2008) Damage characterization of polymer-based composite materials: multivariable analysis and wavelet transform for clustering acoustic emission data. Mech Syst Signal Process 22:1441–1464. https://doi.org/10.1016/j.ymssp.2007.11.029

Martin CA, Van Way CB, Lockyer AJ et al (1995) Acoustic emission testing on an F/A 18 E/F titanium bulkhead. Smart Struct Mater 2444:204–211. https://doi.org/10.1117/12.207672

Martínez-Jequier J, Gallego A, Suárez E et al (2015) Real-time damage mechanisms assessment in CFRP samples via acoustic emission lamb wave modal analysis. Compos Part B Eng 68:317–326. https://doi.org/10.1016/j.compositesb.2014.09.002

McBride SL, MacLachlan JW, Paradis BP (1981) Acoustic emission and inclusion fracture in 7075 aluminum alloys. J Nondestr Eval 2:35–41. https://doi.org/10.1007/BF00614995

McLaskey GC, Glaser SD (2012) Acoustic emission sensor calibration for absolute source measurements. J Nondestruct Eval 31:157–168. https://doi.org/10.1007/s10921-012-0131-2

McLaskey GC, Glaser SD, Grosse CU (2010) Beamforming array techniques for acoustic emission monitoring of large concrete structures. J Sound Vib 329:2384–2394. https://doi.org/10.1016/j.jsv.2009.08.037

Mirgal P, Pal J, Banerjee S (2020) Online acoustic emission source localization in concrete structures using iterative and evolutionary algorithms. Ultrasonics 108:106211. https://doi.org/10.1016/j.ultras.2020.106211

Mistras (2013). 1284: The first multi channel wireless acoustic emission system. [Online] http://www.mistrasgroup.com/products/company/Publications/2$Acoustic_Emission/1284_AE_Wireless_Node.pdf

Moore PO (ed) (2005) Nondestructive testing handbook, acoustic emission testing, vol 6. American Society for Nondestructive Testing

Morscher GN (1999) Modal acoustic emission of damage accumulation in a woven SiC/SiC composite. Vacuum 59:687–697. https://doi.org/10.1016/S0266-3538(98)00121-3

Murray BR, Kalteremidou KA, Carrella-Payan D et al (2020) Failure characterisation of CF/epoxy V-shape components using digital image correlation and acoustic emission analyses. Compos Struct 236. https://doi.org/10.1016/j.compstruct.2019.111797

Nakatani H, Hajzargarbashi T, Ito K et al (2012) Impact localization on a cylindrical plate by near-field beamforming analysis. In: Tomizuka M (ed) Sensors and smart structures technologies for civil, mechanical, and aerospace

Neau G, Deschamps M, Lowe MJS (2001) Group velocity of Lamb waves in anisotropic plates: comparison between theory and experiments. In: AIP conf proc, pp 81–88.

Njuhovic E, Bräu M, Wolff-Fabris F et al (2014) Identification of interface failure mechanisms of metallized glass fibre reinforced composites using acoustic emission analysis. Compos Part B Eng 66:443–452. https://doi.org/10.1016/j.compositesb.2014.06.018

Ohtsu M, Ono K (1984) A generalized theory of acoustic emission and Green's function in a half space. J Acoust Emission 3:27–40

Ohtsu M, Ono K (1986) The generalized theory and source representation of acoustic emission. J Acoust Emission 5:124–133

Ono K (2017) On the piezoelectric detection of guided ultrasonic waves. Materials 10:1325. https://doi.org/10.3390/ma10111325

Ono K, Gallego A (2012) Research and applications of AE on advanced composites. J Acoust Emission 30:180–229

Ospitia N, Aggelis DG, Tsangouri E (2020) Dimension effects on the acoustic behavior of TRC plates. Materials 13:955. https://doi.org/10.3390/ma13040955

Ozevin D, Heidary Z (2011) Acoustic emission source orientation based on time scale. J Acoust Emission 29:123–132

Ozevin D, Greve DW, Oppenheim IJ et al (2006) Resonant capacitive MEMS acoustic emission transducers. Smart Mater Struct 15:1863–1871. https://doi.org/10.1088/0964-1726/15/6/041

Papasalouros D, Bollas K, Kourousis D et al (2016) Acoustic emission monitoring of high temperature process vessels & reactors during cool down, emerging Technologies in non-destructive testing. In: Proceedings of the 6th international conference on emerging technologies in nondestructive testing, ETNDT 2016, VI, pp 197–201

Park WH, Packo P, Kundu T (2017) Acoustic source localization in an anisotropic plate without knowing its material properties – a new approach. Ultrasonics 79:9–17. https://doi.org/10.1016/j.ultras.2017.02.021

Pearson MR, Eaton M, Featherston C et al (2017) Improved acoustic emission source location during fatigue and impact events in metallic and composite structures. Struct Heal Monit 16:382–399. https://doi.org/10.1177/1475921716672206

Philippidis TP, Nikolaidis VN, Anastassopoulos AA (1998) Damage characterisation of C/C laminates using neural network techniques on AE signals. NDT E Int 31:329–340. https://doi.org/10.1016/S0963-8695(98)00015-2

Piotrkowski R, Gallego A, Castro E et al (2005) Ti and Cr nitride coating/steel adherence assessed by acoustic emission wavelet analysis. NDT E Int 38:260–267. https://doi.org/10.1016/j.ndteint.2004.09.002

Pollock AA (1986) Classical wave theory in practical AE testing, In: Proceedings of the 8th international AE symposium. Tokyo, Japan, pp 708–721.

Prieß T, Sause MG, Fischer D et al (2015) Detection of delamination onset in laser-cut carbon fiber transverse crack tension specimens using acoustic emission. J Compos Mater 49:2639–2647. https://doi.org/10.1177/0021998314552003

Prosser WH (1996) Advanced AE techniques in composite materials research. J Acoust Emission 14:1–11. http://ntrs.nasa.gov/search.jsp?R=20040110429

Prosser WH (2002) (Ch. 6) acoustic emission. In: Shull PJ (ed) Nondestructive evaluation, theory, techniques and applications. Marcel Dekker, New York, pp 369–446

Prosser WH et al (1995) Advanced waveform-based acoustic emission detection of matrix cracking in composites. Mater Eval 53:1052–1058

Prosser WH et al (1997) Evaluation of damage in metal matrix composites by means of acoustic emission monitoring. NDT E Int 30:108. https://doi.org/10.1016/S0963-8695(97)85514-4

Prosser WH, Hamstad MA, Gary J et al (1999) Finite element and plate theory modeling of acoustic emission waveforms. J Nondestruct Eval 18:83–90. https://doi.org/10.1023/A:1021888009896

Prosser WH, Gorman MR, Madaras E (2004) Acoustic emission detection of impact damage on space shuttle structures. In: 17th international acoustic emission symposium. https://doi.org/10.1063/1.1916797.

Ramirez-Jimenez CR, Papadakis N, Reynolds N et al (2004) Identification of failure modes in glass/polypropylene composites by means of the primary frequency content of the acoustic emission event. Compos Sci Technol 64:1819–1827. https://doi.org/10.1016/j.compscitech.2004.01.008

Richardson JM, Elsley RK, Graham LJ (1984) Nonadaptive, semi-adaptive and adaptive approaches to signal processing problems in nondestructive evaluation. Pattern Recogn Lett 2:387–394. https://doi.org/10.1016/0167-8655(84)90005-9

Ritschel F et al. (2014) Acoustic emission (AE) signal classification from tensile tests on plywood and layered wood, In: 31st conference of the European working group on acoustic emission. Dresden, Germany, pp 1–7.

Sause M (2010) Identification of failure mechanisms in hybrid materials utilizing pattern recognition techniques applied to acoustic emission signals. mbv-Verlag, Berlin. https://doi.org/10.13140/RG.2.1.4492.2088.

Sause MGR (2013) Acoustic emission signal propagation in damaged composite structures. J Acoust Emission 31:1–18

Sause MGR (2016) In situ monitoring of fiber-reinforced composites. Springer, Cham. https://doi.org/10.1007/978-3-319-30954-5

Sause M, Hamstad M (2018) Acoustic emission analysis. In: Beaumont PWR, Zweben CH (eds) Comprehensive composite materials II. Elsevier, Oxford, pp 291–326. https://doi.org/10.1016/B978-0-12-803581-8.10036-0

Sause MGR, Horn S (2010a) Simulation of acoustic emission in planar carbon fiber reinforced plastic specimens. J Nondestruct Eval 29:123–142. https://doi.org/10.1007/s10921-010-0071-7

Sause MGR, Horn SR (2010b) Influence of specimen geometry on acoustic emission signals in fiber reinforced composites: FEM-simulations and experiments. In: 29th European conference on acoustic emission testing. Vienna, Austria, pp 1–8.

Sause MGR, Richler S (2015) Finite element modelling of cracks as acoustic emission sources. J Nondestruct Eval 34:4. https://doi.org/10.1007/s10921-015-0278-8

Sause MGR, Schultheiß D, Horn S (2008) Acoustic emission investigation of coating fracture and delamination in hybrid carbon fiber reinforced plastic structures. J Acoust Emission 26:1–13

Sause MGR, Haider F, Horn S (2009) Quantification of metallic coating failure on carbon fiber reinforced plastics using acoustic emission. Surf Coatings Technol 204:300–308. https://doi.org/10.1016/j.surfcoat.2009.07.027

Sause MGR, Gribov A, Unwin AR et al (2012) Pattern recognition approach to identify natural clusters of acoustic emission signals. Pattern Recogn Lett 33:17–23. https://doi.org/10.1016/j.patrec.2011.09.018

Sause MGR et al. (2014) Acoustic emission source localization in bearing tests of fiber reinforced polymers by neural networks. In: 16th international conference on experimental mechanics. Cambridge, UK, pp 1–3.

Scholey JJ, Wilcox PD, Wisnom MR et al (2010) Quantitative experimental measurements of matrix cracking and delamination using acoustic emission. Compos A 41:612–623. https://doi.org/10.1016/j.compositesa.2010.01.008

Scruby CB (1985) Quantitative acoustic emission techniques. Non Destructive Test 8:141–208

Sen N, Gawroński M, Packo P et al (2020) Square-shaped sensor clusters for acoustic source localization in anisotropic plates by wave front shape-based approach. Submitted to MSSP 2020

Shen, G. (2017), Progress of acoustic emission technology on pressure equipment in China. Proceedings of the world conference on acoustic Emission-2015. Springer Proceedings in Physics

Surgeon M, Wevers M (1999) Modal analysis of acoustic emission signals from CFRP laminates. NDT E Int 32:311–322. https://doi.org/10.1016/S0963-8695(98)00077-2

Talreja R, Phan N (2019) Assessment of damage tolerance approaches for composite aircraft with focus on barely visible impact damage. Compos Struct 219:1–7. https://doi.org/10.1016/j.compstruct.2019.03.052

Tobias A (1976) Acoustic-emission source location in two dimensions by an array of three sensors. Non Destructive Test 9:9–12ISSN 0029-1021. https://doi.org/10.1016/0029-1021(76)90027-X

Tsangouri E, Aggelis DG (2018) The influence of sensor size on acoustic emission waveforms-a numerical study. Appl Sci 8:168. https://doi.org/10.3390/app8020168

Veloso GFC, Silva LD et al. (2006) Localization of partial discharges in transformers by the analysis of the acoustic emission. In: IEEE international symposium on industrial electronics, pp 537–541

Vergeynst LL et al (2014a) Finite element modelling used to support wood failure identification based on acoustic emission signals. Timber Bridges COST Conf 2014:141–146

Vergeynst LL, Sause MGR, Steppe K (2014b) Acoustic emission signal detection in drought-stressed trees: beyond counting hits. In: 31st Conference of the European working group on acoustic emission. Dresden, Germany, pp 1–8.

Vi-Tong E, Gaillard P (1987) An algorithm for non-supervised sequential classification of signals. Pattern Recogn Lett 5:307–313. https://doi.org/10.1016/0167-8655(87)90071-7

Wadley HNG, Scruby CB (1981) Acoustic emission source characterization. Advances in acoustic emission. Dunhart Publishers, Knoxville

Wang Y-B, Chang D-G, Fan Y-H et al (2017) Acoustic localization of partial discharge sources in power transformers using a particle-swarm-optimization-route-searching algorithm. IEEE Trans Dielect Electr Insul 24:3647–3656. https://doi.org/10.1109/TDEI.2017.006857

Ward IM (1971) Mechanical properties of solid polymers. John Wiley & Sons Ltd., New York

Wevers M (1997) Listening to the sound of materials: acoustic emission for the analysis of material behaviour. NDT E Int 30:99–106. https://doi.org/10.1016/S0963-8695(96)00051-5

Wilcox PD et al (2006) Progress towards a forward model of the complete acoustic emission process. Adv Mater Res 13–14:69–75

Wild, G., Hinckley, S. (2008) Acousto-Ultrasonic Optical Fiber Sensors: Overview and State-of-the-Art. IEEE Sensors Journal, Vol. 8, No. 7, 1184–1193

Wisner B, Kontsos A (2018) Investigation of particle fracture during fatigue of aluminum 2024. Int J Fatigue 111:33–43. https://doi.org/10.1016/j.ijfatigue.2018.02.001

Wisner BJ, Potstada P, Perumal VI et al (2019) Progressive failure monitoring and analysis in aluminium by in situ nondestructive evaluation. Fatigue Fract Eng Mater Struct 42:2133–2145. https://doi.org/10.1111/ffe.13088

Wolfe JP (2005) Imaging phonons: acoustic wave propagation in solids. Cambridge University Press, Cambridge

Wu Q, Okabe Y (2012) Novel acoustic emission sensor system based on two cascaded phase-shifted fiber Bragg gratings. In: Proceedings of the SPIE international conference fiber sensation, p 8421

Xiao D, He T, Pan Q et al (2014) A novel acoustic emission beamforming method with two uniform linear arrays on plate-like structures. Ultrasonics 54:737–745. https://doi.org/10.1016/j.ultras.2013.09.020

Yao WB, Dai CY, Mao WG et al (2012) Acoustic emission analysis on tensile failure of air plasma-sprayed thermal barrier coatings. Surf Coatings Technol 206:3803–3807. https://doi.org/10.1016/j.surfcoat.2012.03.050

Yedavalli RK, Belapurkar RK (2011) Application of wireless sensor networks to aircraft control and health management systems. J Control Theory Appl 9:28–33

Yin S, Cui Z, Kundu T (2018) Acoustic source localization in anisotropic plates with "Z" shaped sensor clusters. Ultrasonics 84:34–37. https://doi.org/10.1016/j.ultras.2017.10.007

Yu P, Anastassopoulos V, Venetsanopoulos AN (1996) Pattern recognition based on morphological shape analysis and neural networks. Math Comput Simul 40:577–595. https://doi.org/10.1016/0378-4754(95)00008-9

Zhou W, Qin R, Han K-N, Wei Z-Y, Ma L-H (2021) Progressive damage visualization and tensile failure analysis of three-dimensional braided composites by acoustic emission and micro-CT. Polym Test 93:106881. https://doi.org/10.1016/j.polymertesting.2020.106881